

Supplementary Materials for
The PET tracer [¹¹C]MODAG-005 targets alpha-synuclein aggregates in
the brain

Ran Sing Saw *et al.*

Corresponding author: Christian Griesinger, cigr@mpinat.mpg.de; Armin Giese, giese@modag.net;
Kristina Herfert, kristina.herfert@med.uni-tuebingen.de

Sci. Transl. Med. **18**, eaec0813 (2026)
DOI: 10.1126/scitranslmed.aec0813

The PDF file includes:

Materials and Methods
Figs. S1 to S21
Tables S1 to S3
References (42–52)

Other Supplementary Material for this manuscript includes the following:

Data files S1 and S2
MDAR Reproducibility Checklist

Supplementary Materials

Materials and Methods

Precursor and standard synthesis of MODAG-005

All starting materials and solvents were of commercial grade and used as received unless noted otherwise. Thin layer chromatography (TLC): Macherey-Nagel precoated sheets, 0.25 mm ALUGRAM® SIL G/UV254 plates, detection with UV or by charring with 10% w/w ethanolic phosphomolybdic acid reagent, or both, followed by heating at 200°C. Flash column chromatography was performed by using Merck silica gel 60 (0.063-0.100 mm). Analytical high-performance liquid chromatography (HPLC) was performed by using a Waters HPLC system with a Waters 996 Photodiode Array Detector. All separations involved a mobile phase of 0.1% trifluoroacetic acid (TFA) (v/v) in water and 0.1% TFA in acetonitrile. Unless otherwise specified, a gradient of 50% CH₃CN /50% H₂O → 100% CH₃CN in 30 minutes was used. HPLC was performed by using a reversed-phase (RP) column Eurospher RP 18, 100 Å, 5 µm, 250 × 4.6 mm at a flow rate of 1 mL/min. Electrospray ionization mass spectrometry (ESI-MS) and liquid chromatography/mass spectrometry (LC/MS) analyses were obtained by using a Waters Micromass ZQ 4000 mass spectrometer in conjunction with the Waters HPLC apparatus described above. NMR spectra were recorded by using a 400 MHz Bruker Avance spectrometer (Bruker AG, Rheinstetten, Germany) equipped with a TXI HCN z-gradient probe. All spectra were processed by using TOPSPIN 3.1 (Bruker AG, Karlsruhe, Germany). ¹H-NMR chemical shifts (δ) are reported in parts per million (ppm) relative to DMSO-d₅ as an internal standard. Data are reported as follows: chemical shift, multiplicity (s = singlet, bs = broad singlet, d = doublet, dd = doublet of doublets, ddd = doublet of doublet of doublets), coupling constants (J, given in Hz), integration. ¹³C-NMR chemical shifts (δ) are reported in parts per million (ppm) relative to DMSO-d₆ as an internal standard. The following experiments were used to record the resonances of the compounds: ¹H-1D, ¹³C-1D-NMR spectra and ¹³C-APT (attached proton test with a single J-evolution time of 1/145 seconds, spectra are processed such that quaternary and methylene groups have positive sign and methyl and methine groups negative sign). To resolve the overlap of resonances and recover undetectable resonances in ¹H and APT spectra, 2D-[¹³C, ¹H]-HSQC (heteronuclear single quantum coherence), 2D-[¹³C, ¹H]-HMBC (heteronuclear multiple bond correlation) and 2D-NOESY were recorded for some compounds. The synthesis of the precursor anle190214 is depicted in Fig. S22.

The calculated logP (clogP) and topological polar surface area (tPSA, [Å²]) values shown in **Fig. S20** were calculated by the Molinspiration property engine (v2021.10).

Experimental procedures and characterization data of compounds

MODAG-005:

4-[5-(2-Bromopyridin-4-yl)-1H-pyrazol-3-yl]-N-methylaniline was synthesized as described previously (14).

tert-Butyl {4-[3-(2-bromopyridin-4-yl)-3-oxopropanoyl]phenyl} carbamate **3**:

A solution of potassium *tert*-butoxide (FW 112.21, 583 mg, 5.2 mmol) in THF (10.4 mL) was added to a stirred solution of *tert*-butyl *N*-(4-acetylphenyl)carbamate **1** (FW 235.28, 941 mg, 4 mmol) and methyl 2-bromopyridine-4-carboxylate **2** (FW 216.03, 1.04 g, 4.8 mmol) in THF (15 mL). The reaction mixture was stirred for 20 h. A 10 μ L aliquot was sampled, quenched with 1M phosphate buffer pH 7, extracted with EtOAc and analyzed by TLC and LC-MS. About 95% conversion of ketone was observed. The mixture was poured into 1M phosphate buffer pH 7 (15 mL) and ice water (15 mL), and stirred at 0°C for 30 min. The resulting yellow solid was filtered off, washed with water (3 \times 10 mL) and air dried to give 1.57 g (3.74 mmol, 94%) of crude product, which was used for the next step w/o purification. LC-MS: sample 0.5 mg/mL in CH₃CN; 10 μ L injection volume; column: Eurospher RP18 100 Å, 5 μ m, 250 \times 4.6 mm, solvents: water (+0.1% TFA, A) and CH₃CN (+0.1% TFA, B), gradient: B 50% \rightarrow 100% in 30 min, detector UV 260 nm, peak RT 22.9 min, mass 419.2 (100%), 421.2 (98%), [M+H]⁺. TLC (SiO₂, *n*-hexane:EtOAc = 2:1), R_f = 0.7.

tert-Butyl {4-[5-(2-bromopyridin-4-yl)-1*H*-pyrazol-3-yl]phenyl} carbamate **4**:

To a solution of the *tert*-butyl {4-[3-(2-bromopyridin-4-yl)-3-oxopropanoyl]phenyl} carbamate **3** (1.57 g, 3.74 mmol) in THF (20 mL) was added hydrazine monohydrate (388 μ L, 400 mg, 8 mmol). After being stirred at 50°C for 24 h the reaction mixture was cooled to room temperature and concentrated under reduced pressure. A mixture *n*-hexane/EtOAc = 2/1 (16 mL) was added, the mixture was stored 2 h at room temperature, then 15 h at 4°C. The resulting solid was filtered off, washed with *n*-hexane and vacuum dried. The crude product was purified by flash chromatography on silica gel (*n*-hexane/EtOAc = 1/1) to afford 1.18 g (2.84 mmol, 76%) of title product as beige solid. ¹H NMR (400 MHz, DMSO-d₆, two rotamers, main form) δ = 13.63 (bs, 1H), 9.53 (s, 1H), 8.41 (d, *J* = 5.1 Hz, 1H), 8.02 (s, 1H), 7.86 (d, *J* = 5.1 Hz, 1H), 7.69 (d, *J* = 8.6 Hz, 2H), 7.57 (d, *J* = 8.6 Hz, 2H), 7.35 (s, 1H), 1.49 (s, 9H). ¹³C NMR (100.6 MHz, DMSO-d₆, two rotamers, main form) δ = 152.8, 150.9, 147.6, 144.2, 142.3, 139.2 (2C), 125.8 (2C), 123.2, 122.6, 119.2, 118.4 (2C), 100.6, 79.4, 28.2 (3C). LC MS (RP18-100 Å, gradient 50% CH₃CN /50% H₂O \rightarrow 100% CH₃CN in 30 min), RT 14.6 min and mass 415.3 (100%), 417.3 (98%), [M+H]⁺. TLC (SiO₂, *n*-hexane/EtOAc = 1/1) R_f 0.56, m.p.: 230-235°C (dec).

4-[5-(2-bromopyridin-4-yl)-1*H*-pyrazol-3-yl]aniline **anle190214**:

To a suspension of *tert*-butyl {4-[5-(2-bromopyridin-4-yl)-1*H*-pyrazol-3-yl]phenyl} carbamate **4** (FW 415.28, 1.18 g, 2.84 mmol) in CH₂Cl₂ (21 mL) trifluoroacetic acid (2.8 mL, 4.14 g, 36.4 mmol) was added. The mixture was stirred at room temperature for 15 h and concentrated in vacuum. 1M phosphate buffer pH 7 (20 mL) was added, the resulting precipitate was filtered off, washed with water (2 \times 10 mL) and air dried to give 859 mg (2.73 mmol, 96%) of product as a yellow-orange colored solid. ¹H NMR (400 MHz, DMSO-d₆) δ = 13.22 (bs, 1H), 8.39 (d, *J* = 5.2 Hz, 1H), 8.01 (d, *J* = 0.8 Hz, 1H), 7.83 (dd, *J* = 5.2, 1.4 Hz, 1H), 7.47 (ddd, *J* = 7.5, 1.7, 0.9 Hz, 2H), 7.19 (s, 1H), 6.64 (ddd, *J* = 7.5, 1.7, 0.9 Hz, 2H), 5.49 (bs, 2H). ¹³C NMR (100.6 MHz, DMSO-d₆) δ = 150.8, 149.2, 146.4, 146.1, 143.8, 142.2, 126.3 (2C), 123.0, 119.0, 116.8, 113.9 (2C), 99.2. LC MS (RP18-100Å, gradient 0% CH₃CN /100% H₂O \rightarrow 100% CH₃CN in 30 min), RT 14.8 min and mass 315.2 (98%), 317.2 (100%), [M+H]⁺. TLC (SiO₂, *n*-hexane/EtOAc = 1/1) R_f 0.25, m.p.: >300°C.

MODAG-005 tritiation

MODAG-005 was tritiated (RC Tritec AG, Teufen Switzerland), dissolved in EtOH, and stored at -80°C until further usage. The molar activity (A_m) was $2.96\text{ GBq}/\mu\text{mol}$, and its radiochemical purity was $>98\%$, as determined through HPLC.

Fibril generation

Expression, purification, and generation of sonicated human recombinant wild-type alpha-synuclein (α -Syn) were performed using previously established protocols (14, 15). Carrier-free recombinant human 4-repeat-tau (4R-tau) (Tau-441/2N4R-Tau), hereinafter referred to as tau, was purchased lyophilized from Bio-Techne GmbH (Wiesbaden, Germany), and reconstituted in 50 mM Tris-buffer, pH 7.0. Fibrillation was induced by heparin under constant agitation and the generated fibrils were sonicated, as described previously (14, 42).

Sonicated amyloid-beta 1-42 ($A\beta_{1-42}$) fibril production was adapted from (29) and performed as described previously (14), but with 96-hour incubation time. Validation was performed using thioflavin T (ThT) fluorescence assay, negative staining transmission electron microscopy, as described previously (14), as well as [^3H]Pittsburg compound B (PiB) saturation binding assay (Fig. S17). Prior to binding experiments, the optimal concentration for the respective fibril type was determined by performing a concentration determination assay to prevent ligand depletion, as described in (14).

Fibril binding experiments

Filtration and readout of fibril binding experiments were performed as previously described (14). Briefly, for competition binding experiments, a fixed concentration of α -Syn (15 nM) fibrils was incubated with 1 nM [^3H]MODAG-001 in low-binding plates (96-well micro test plate, ratilab GmbH, Dreieich, Germany). Competition was induced by adding ten concentrations of a 1:4 serial dilution of unlabeled MODAG-005 ($4\text{ }\mu\text{M}$ – 0.02 nM) in 30 mM Tris-HCl, 10% ethanol, 0.05% Tween20, pH 7.4 (in the following referred to as EtOH-Tween buffer) in a total volume of $200\text{ }\mu\text{L}/\text{well}$.

For [^3H]MODAG-005 saturation binding assays, a fixed concentration of α -Syn (15 nM), tau (250 nM) or $A\beta_{1-42}$ ($1\text{ }\mu\text{M}$) fibrils was incubated with decreasing concentrations of [^3H]MODAG-005 ($6\text{ nM}/24\text{ nM}$ – 0.05 nM) in EtOH-Tween buffer in a total volume of $200\text{ }\mu\text{L}/\text{well}$. Co-incubation with 400 nM unlabeled MODAG-005 was used to determine non-specific binding of the radiotracer. For [^3H]PiB saturation binding assay, $A\beta_{1-42}$ ($2.5\text{ }\mu\text{M}$) fibrils was incubated with decreasing concentrations of [^3H]PiB (32 nM – 0.06 nM) in 50 mM Tris-HCl, 10% EtOH, 0.1% BSA, 0.025% NaN_3 , pH 7.4, in a total volume of $200\text{ }\mu\text{L}/\text{well}$. Co-incubation with 400 nM unlabeled PiB was used to determine non-specific binding of the radiotracer.

Incubation at 45 rpm for two hours at 37°C was performed on a shaker (MaxQ™ 6000, orbit diameter 1.9 cm , Thermo Fisher Scientific Inc., Marietta, OH, USA). A filtermat harvester (PerkinElmer, Waltham, MA, USA) was used to filter bound radioligands onto a glass fibre filtermat B (PerkinElmer, Waltham, MA, USA), which was pre-incubated with $5\text{ mg}/\text{mL}$ polyethyleneimine (Sigma Aldrich Chemie GmbH, Taufkirchen, Germany) only for α -Syn and $A\beta_{1-42}$ fibrils. After harvesting, the filtermat was dried in the microwave, and melt-on scintillator sheets (MeltiLex™ B/HS, PerkinElmer, Waltham, MA, USA) were molten into the filtermat. After solidification at room temperature, the filter was placed in a MicroBeta sample bag (PerkinElmer, Waltham, MA, USA) and measured using the Wallac MicroBeta® TriLux liquid scintillation counter (PerkinElmer, Waltham, MA, USA).

Radioactivity converted to bound pmol fibril per added nmol of total fibril was plotted against increasing [³H]MODAG-005 or [³H]PiB concentrations in nM. Data points were fitted using nonlinear regression analysis in GraphPad Prism (GraphPad Software, Inc., Version 7.03, La Jolla (CA), USA). Saturation binding assays were performed in triplicates and repeated in three independent experiments.

Off-target binding

A Cerep diversity panel and a customized kinase panel assay were performed by Eurofins Cerep in France with a specific focus on monoamine oxidase B (MAO-B) binding. The compound enzyme inhibition effect was calculated as a % inhibition of control enzyme activity. Competition binding assays were performed using increasing concentrations of MODAG-005 and IC₅₀ values were determined by non-linear regression analysis of the competition curves.

Human and mouse brain tissue

Post-mortem human brain tissue samples were provided as 10 μm sections by the Neurobiobank Muenchen (NBM, Munich, Germany), where cases were collected on the basis of written informed consent according to the guidelines of the ethics committee of the Ludwig-Maximilians-University Munich, Germany (# 345-13). **Table S1** provides a summary of the patients and controls from which brain tissues were obtained. For Parkinson's disease (PD) case, the disease duration was approximately 25–26 years, with the first symptoms appearing in the patient's mid-60s as tremor of the left hand. The disease progressed with exhibition of akinetic-rigid syndrome and camptocormia over time, as well as mild cognitive impairment ten years ante mortem, and dementia (PD with dementia) five years ante mortem. The use of human tissue samples for this study was approved by the ethics committee of the Faculty of Medicine at the University of Tuebingen (Ethics approval number: 813/2018BO2).

In addition, 20 μm sagittal mouse brain sections for autoradiography experiments were obtained from an α-Syn(A30P) (B6.Cg-Tg(THY1-SNCA A30P)1734Sud/J) and an age-matched wild-type (male, 72 weeks) mouse. All tissues were stored at -80°C until further use.

***In vitro* autoradiography**

Post-mortem human and mouse brain sections were used for autoradiographic evaluation of [³H]MODAG-005. After defrosting, the brain sections were pre-incubated in 30 mM Tris-HCl, 0.1% bovine serum albumin (BSA), pH 7.4 (in the following referred to as BSA buffer) for 25 minutes at room temperature. For total binding, the sections were incubated in 3 nM [³H]MODAG-005. For blocking, adjacent sections were co-incubated with 3 μM unlabeled MODAG-005 or anle138b.

For saturation binding experiments, brain sections were incubated with decreasing concentrations of [³H]MODAG-005 (48 to 0.1 nM for MSA; 96 to 0.2 nM for AD). To determine non-specific binding, adjacent sections (for tracer concentrations 96 nM, 48 nM, 24 nM, and thereafter every second section) were co-incubated with 3 μM unlabeled MODAG-005. In the selegiline pre-blocking saturation experiment, MSA tissue sections were pre-incubated in 3 μM selegiline for one hour at room temperature and washed (three times for ten minutes) before tracer incubation (96 to 0.38 nM, with non-specific binding determined at every tracer concentration). For competition binding experiments, 1 nM [³H]MODAG-005 was incubated with decreasing concentrations of unlabeled anle138b (2 μM to 0.03 nM).

In all experiments, brain sections were incubated at room temperature for one hour with subsequent washing in ice-cold BSA buffer (three times for ten minutes) followed by dipping for three seconds in ice-cold deionized water. The dried sections were then exposed to a phosphor imaging plate (BAS-IP TR2025, Fuji Imaging Plate, VWR, Denmark) with a tritium standard (ART-123 and ART-123A; American Radiolabelled Chemicals, St. Louis, MO, USA) for seven days and scanned in a phosphor imager (BAS 5000, FUJIFILM Life Science, Stamford, CT, USA).

For data quantification, ImageJ software (US National Institutes of Health, Bethesda, MD, USA) was used. Images were converted to 32-bit and the square math function for increasing the grey value range was applied. Regions of interest (ROIs) were drawn over the tritium standard to obtain a standard curve. ROIs were placed in the white matter of multiple system atrophy (MSA), progressive supranuclear palsy (PSP), a neurodegenerative tauopathy with a predominance of 4R-tau isoforms (43), and control cases (cerebellum and frontal cortex), and in the grey matter of PD, Alzheimer's disease (AD), and control cases (frontal cortex). For the mouse brain sections, ROIs were placed in the midbrain, brainstem, zona incerta, cortex, and cerebellum (**Fig. S5**), which are brain regions of expected α -Syn pathology, and cross-validated with pSer129 α -Syn immunofluorescence microscopy (32). Specific binding was calculated by subtracting the non-specific binding from the total binding values. After interpolation from the standard curve, the specific binding values were divided by the A_m of the tracer and converted into fmol/mg.

Statistical analysis was performed using GraphPad Prism (Version 8.4.0). Comparisons were carried out using values obtained from repeated measurements in each sample (ROIs placed at different locations) to capture any difference in pathology and tracer binding across the tissue sections. Welch's t-test was used to compare the specific binding between MSA cases and controls (cerebellum - white matter), as well as PSP and control (frontal cortex - white matter). For comparison of AD and PD with control (frontal cortex - grey matter), Brown-Forsythe and Welch ANOVA with Dunnett's T3 multiple comparisons test was carried out. For the saturation binding experiments, a Scatchard plot was prepared in GraphPad Prism based on the calculated specific binding. Data points for the high-affinity binding site and the low-affinity binding site were determined by visual inspection. Subsequently, non-linear regression (saturation binding: one-site - total and non-specific binding) was performed independently for the two sites to determine the respective K_d and B_{max} values. The lines in the Scatchard plot were drawn based on these values, where x-intercept = B_{max} and y-intercept = B_{max}/K_d . For the competition experiment with anle138b in MSA, non-linear regression (competitive binding: one-site-fit K_i) was used. For the autoradiography in mouse brain tissues, no statistical test was performed.

Microautoradiography

For microscopic investigation of tracer binding, microautoradiography was performed. Tissues were thawed and fixed in 4.5% paraformaldehyde (PFA, SAV Liquid Production GmbH, Flintsbach am Inn, Germany) for ten minutes at room temperature. Pre-incubation and washing steps were as above. Brain sections were incubated for one hour with 30 or 60 nM [3 H]MODAG-005. Adjacent tissue sections were additionally incubated with 30 μ M unlabeled MODAG-005, anle138b, or selegiline for blocking. Subsequent procedures were performed in a safe light-illuminated dark room. The slides were dipped for five seconds into a 1:1 mixture of distilled water and Ilford K5 emulsion (Agar Scientific Ltd, Stansted, UK) molten in a 40°C water bath and left to dry in an upright position for two hours at room temperature. After drying,

the slides were stored in the dark at 4°C for one to two weeks. For development, the slides were incubated for four minutes in Ilford Phenisol at 20°C, followed by one minute in Ilford Ilfostop and four minutes in Ilford Hypam (prepared according to manufacturer's instruction, Agar Scientific Ltd, Stansted, UK). The slides were then washed in running tap water for ten minutes and finally rinsed in distilled water.

Immunofluorescence

Immunofluorescence microscopy was carried out on the same brain sections after (micro)autoradiography. All sections were fixed with 4.5% PFA as above, when not performed prior to microautoradiography. For antigen retrieval, sodium citrate buffer (10 mM, pH 6.0, Sigma Aldrich Chemie GmbH, Darmstadt, Germany) was boiled and the brain sections to be stained for α -Syn pSer129 and phospho-tau (pTau) were incubated at room temperature in the boiled buffer for 30 minutes; brain sections to be stained for A β ₁₋₄₂ were incubated in 97% formic acid for ten minutes at room temperature. After washing, the sections were subsequently equilibrated in Tris-buffered saline (TBS) supplemented with 0.1% Triton X-100 and 1% BSA, pH 7.6 (in the following referred to as TBS-X) for ten minutes, before blocking in TBS supplemented with 0.3% Triton X-100 and 10% normal goat serum (Vector Laboratories, Linaris Biologische Produkte GmbH, Dossenheim, Germany) for 60 minutes at room temperature. Incubation with primary antibody was carried out overnight at 4°C with either mouse anti-phosphorylated α -Syn pSer129 monoclonal antibody (1:5000 in TBS-X, pSyn#64; 015-25191, FUJIFILM Wako Chemicals Europe GmbH, Neuss, Germany), mouse anti-pTau (Ser202, Thr205) monoclonal antibody (1:500 in TBS-X, AT8, MN1020, Invitrogen, Rockford, IL, USA), or rabbit anti-A β ₁₋₄₂ polyclonal antibody (1:200 in TBS-X, 218703, Synaptic Systems, Goettingen, Germany). After three times washing with TBS-X, the sections were incubated with secondary antibodies (1:250 in TBS-X) for one hour in the dark, using either goat anti-mouse Alexa Fluor 488 (A-11036, Invitrogen, Carlsbad, CA, USA), goat anti-mouse Alexa Fluor 647 (A32728, Invitrogen, Carlsbad, CA, USA), or goat anti-rabbit Alexa Fluor 568 (A-11036, Invitrogen, Carlsbad, CA, USA). After three washes following secondary antibody incubation, sections were stained with 3 nM 4',6-diamidino-2-phenylindole (DAPI) (Invitrogen, Carlsbad, CA, USA) for five minutes and washed before being mounted on coverslips with ProLong Glass Antifade Mountant (Invitrogen, Carlsbad, CA, USA).

Whole-section images of the stained tissues were captured at 10 \times magnification using Leica DMI8 microscope interfaced with Leica LAS X software (Leica Microsystems CMS GmbH, Wetzlar, Germany). The images were further processed with ImageJ. Background subtraction was performed with a rolling ball radius of 100 pixels for α -Syn pSer129 and pTau staining, whereas a radius of 200 pixels was used for A β ₁₋₄₂ staining.

For the correlative analysis of autoradiography and immunofluorescence microscopy in PD tissues, the immunofluorescence microscopy image was co-registered with the autoradiography image using the ImageJ plugin 'Big Warp'. Autoradiography images were processed and quantified as above. ROIs of 20 \times 20 pixels were drawn covering the whole brain section. The same ROIs were applied for the co-registered immunofluorescence microscopy image. Mean grey values of the immunofluorescence microscopy image were measured and normalized by dividing them by maximum intensity. Correlation and linear regression analysis of the autoradiography and immunofluorescence microscopy were performed using GraphPad Prism software.

Immunohistochemistry

Immunohistochemistry of α -Syn pSer129, glial fibrillary acidic protein (GFAP), and MAO-B was performed in brain tissue sections from human MSA cases, fibril-injected and non-injected rats, as well as α -Syn(A30P) and wild-type mice from *in vivo* PET study. Thawing, post-fixation (20 minutes) and antigen retrieval of the cryosections were performed as described in the immunofluorescence. Following antigen retrieval, the tissue sections underwent quenching (1 mL quenching solution = 890 μ L TBS, 100 μ L methanol, and 10 μ L 30% hydrogen peroxide) for 20 minutes to inhibit endogenous peroxidase. Following equilibration in buffer and one-hour blocking (0.3% Triton-X and 10% normal goat serum), mouse and rat tissues underwent an additional one-hour blocking step with goat F(ab) anti-mouse or anti-rat IgG (1:100 in TBS-X, ab6668 and ab7172, Abcam, Rozenburg, The Netherlands), respectively, to reduce background. Following F(ab) IgG blocking, tissues were washed for ten minutes in TBS-X. Incubation with primary antibody was carried out overnight at 4°C with either mouse anti-phosphorylated α -Syn (pSer129) monoclonal antibody (1:5000 in TBS-X, pSyn#64; 015-25191, FUJIFILM Wako Chemicals Europe GmbH, Neuss, Germany), rabbit recombinant anti-GFAP antibody (1:1000 in TBS-X, EPR1034Y, Abcam, Rozenburg, The Netherlands) or rabbit polyclonal anti-MAO-B (1:2000 (for human tissue) or 1:2500 (for rodent tissue) in TBS-X, HPA002328, Atlas Antibodies, Bromma, Sweden). Following overnight incubation, tissues were washed three times with TBS-X and incubated with a secondary antibody (EnVision+/HRP Dual Link Rabbit/Mouse, K406189-2, Agilent, Waldbronn, Germany) for 30 minutes at room temperature. After washing, tissues were incubated with 3,3'-diaminobenzidine (1:50 in substrate buffer according to manufacturer's instruction, Agilent, Waldbronn, Germany) for up to ten minutes or NovaRED Substrate Kit (prepared according to manufacturer's instruction by Vector Laboratories, SK-4800, Biozol, Eching, Germany) for up to 20 minutes. Tissues were washed, dehydrated in an ethanol series, and cleared with Clear-Rite 3 (EpreDia Netherlands B.V., DA Breda, Netherlands). Stained tissues were mounted with Eukitt quick-hardening mounting medium (Fluka Analytical, Munich, Germany) and scanned with a NanoZoomer 2.0 HT (Hamamatsu Photonics K.K., Hamamatsu, Japan) at 40 \times magnification.

Semi-quantitative analysis by image thresholding was performed for the immunohistochemistry of α SYN pSer129 in the brainstem of α SYN(A30P) and wild-type mice from *in vivo* PET study. Stained tissues which presented with artifacts not feasible to be removed manually were excluded from analysis. All α SYN(A30P) mice (n = 14, 6–10 tissue sections per animal) and randomly selected wild-type mice (n = 5, 2 tissue sections per animal) were analyzed. ROI was drawn in the brainstem using QuPath (Version 0.4.2). Tissue border and any tissue artifacts were not included into the ROI to avoid staining artifacts. Images with the ROI were exported from QuPath to ImageJ with no pixel downsampling (resolution = 1) and subsequently converted to 8-bit images. A threshold of 0–120 was applied using the “Threshold” function of ImageJ to create binary images and the percentages positive area were measured. Furthermore, qualitative scoring was performed for the immunohistochemistry of MAO-B in α SYN(A30P) and wild-type mice from *in vivo* PET study. Two wild-type mice and two α SYN(A30P) mice were selected from each animal group based on the pathology load (> 5%, 1–5% and < 1% α SYN pSer129) determined by semi-quantitative analysis of α SYN pSer129 immunohistochemistry (4 tissue sections per animal). Staining in the brainstem, midbrain and hypothalamus was given a score from zero to three, where score zero depicted the absence of staining and score three represented the maximum staining which was observed across the stained tissues.

Radiosynthesis of [¹¹C]MODAG-005

Both the precursor anle190214 and the unlabeled reference compound were obtained as above in “Precursor and Standard synthesis of MODAG-005”. All solvents and reagents were obtained by commercial suppliers with analytical grade and used without further purification.

Radiolabeling was carried out by either reductive methylation with [¹¹C]CH₂O or direct methylation using [¹¹C]MeOTf (14, 44), to achieve highly selective labeling of the aniline nitrogen without loss of radioactivity through pyrazole-labelled side product formation, as well as a higher molar activity for *in vivo* binding experiments.

Radiosynthesis by reductive methylation: [¹¹C]CO₂ was prepared by the bombardment of ¹⁴N target gas containing 1% O₂ with 70 μA of 16.5 MeV protons on a PETtrace 890 cyclotron (GE Healthcare). No carrier added [¹¹C]CO₂ was delivered to the automatic synthesis module and [¹¹C]MeI was produced through the gas-phase conversion pathway (8). Radiosynthesis, purification, and formulation were automated on Tracerlab FX MeI and Tracerlab FX M (GE Healthcare) radiochemical synthesizers. Analytical HPLC was performed using an Infinity 1260 HPLC system (Agilent Technologies) equipped with a NaI(Tl) detector for radioactivity detection. Radiochemical and chemical purities of the radiolabeled compound as well as carrier content for calculation of molar radioactivity were determined by analytical radio-HPLC. Briefly, [¹¹C]MeI was trapped in a solution of 1 mg anle190214 and 5 mg trimethylamine *N*-oxide in 350 μL diethyl formamide (DEF) and reacted for three minutes at 60°C. The Schiff-base intermediate was then reduced to [¹¹C]MODAG-005 by the addition of 1.2 mL 0.1 M citrate-phosphate buffer pH 5 containing 60 μL 2 M sodium cyanoborohydride in DEF and incubation for five minutes at 100°C. The product was purified by isocratic HPLC (Phenomenex Synergi Max-RP, 4 μm, 80 Å, 250 × 10 mm; 6 mL/min 55% acetonitrile in water; retention time seven minutes) and reformulated in 500 μL ethanol and 5 mL phosphate-buffered saline (PBS) using a Sep-Pak Plus Light C18 cartridge (Waters, Eschborn, Germany). Radiochemical purity as well as carrier content for calculation of A_m were quantified by analytical HPLC (Phenomenex Luna Phenyl-Hexyl, 5 μm, 100 Å, 250 × 4.6 mm; 1.5 mL/min 30% acetonitrile). At the end of the synthesis (EOS), the radiochemical yield was 12.0 ± 2.2% and the A_m was 49.2 ± 11.2 GBq/μmol. As the obtained A_m at the end of the synthesis was relatively low, further optimization was thus required for successful imaging of low-abundant targets such as α-Syn aggregates for *in vivo* studies.

Radiosynthesis by direct methylation - method A: [¹¹C]MeI was obtained as above in “Radiosynthesis by reductive methylation”. [¹¹C]MeOTf was generated by the reaction of the produced [¹¹C]MeI with silver triflate in an online flow-through process at 200°C under helium gas flow. The radiolabeling precursor anle190214 (1-2 mg, 3.17-6.35 μmoles) was dissolved in 500 μL of 2-butanone and the reaction vial was vortexed. No-carrier added [¹¹C]MeOTf was bubbled through the solution cooled to -20°C. The reaction mixture was heated to 75°C for two minutes. After cooling down to room temperature, the solution was diluted with 1.5 mL of H₂O and transferred to the HPLC system. The crude product purified by semi-preparative HPLC on a Synergi 4 μm Max-RP 80 Å, 250 × 100 mm column was eluted with an isocratic flow of 55% acetonitrile in water (flow rate: 6 mL/min) with a retention time of 6.5 minutes. Chromatograms were registered using an UV-detector (254 nm) and a Geiger-Müller tube. The HPLC fraction containing the purified product was diluted with 50 mL of water and loaded on a Sep-Pak Plus Light C18 cartridge, previously conditioned with 10 mL of ethanol and 10 mL of water. The cartridge was washed with 5 mL of water, and the product was eluted with 0.5 mL of ethanol and

formulated with the addition of 5 mL of PBS. Radiochemical and chemical purities of the radiolabeled compound as well as carrier content for calculation of molar radioactivity were determined by analytical radio-HPLC. At the EOS the radiochemical yield was $11.8 \pm 2.7\%$ and the A_m was 209 ± 44 GBq/ μ mol.

Radiosynthesis by direct methylation - method B: For the *in vivo* studies in macaque, the direct methylation synthesis route, established in the Department of Preclinical Imaging and Radiopharmacy (Tuebingen, Germany), was adapted at Invicro-London and further adapted at Charles River. [^{11}C]CO₂ was produced through a $^{14}\text{N}[\text{p},\alpha]^{11}\text{C}$ nuclear reaction on a Siemens RDS-111 cyclotron, using 1% O₂ in N₂ as the target gas, using a Havar HP target. No carrier-added [^{11}C]CO₂ was delivered to Tracerlab FX₂MeI (GE Healthcare) and [^{11}C]MeI was produced through the gas-phase conversion pathway. [^{11}C]MeI passed through a silver triflate column, packed with a mixture of silver triflate and Carbosphere, at 200°C to generate [^{11}C]MeOTf, which bubbled into a reactor vessel pre-charged with a solution of anle190214 (2–3 mg) in anhydrous acetone (500 μ L) held at -20°C. Radiosynthesis, purification and formulation were automated on EZ Modular Lab radiochemical synthesizers (Eckert & Ziegler GmbH). The reaction mixture was heated to 50°C for three minutes, and then diluted with 1.7 mL of the preparative HPLC eluent. [^{11}C]MODAG-005 was purified by semi-preparative HPLC on an Agilent SB-phenyl column (5 μ m, 9.4 \times 250 mm) with 55% of 95/5 of acetonitrile/H₂O and 45% 50 mM aqueous ammonium acetate solution at a flow rate of 8 mL/min, which was eluted at seven minutes. The quality control of a dose solution was performed with an analytical HPLC on an Agilent SB-phenyl column (5 μ m, 4.6 \times 150 mm) with acetonitrile/50 mM aq. ammonium acetate (45/55) at a flow rate of 1.5 mL/min [^{11}C]MODAG-005 was eluted at 4.3 minutes, which was confirmed by co-injection of a MODAG-005 standard solution, and the radiochemical purity of a dose solution was >98%. At the end of the synthesis, the radiochemical yield (decay-corrected) was $3.7 \pm 2.3\%$ and the A_m was 89.3 ± 14 GBq/ μ mol.

Animals

Mouse and rat experiments were conducted in compliance with the European directives on the protection and use of laboratory animals (Council Directive 2010/63/UE) and with the German animal protection law and with the approval of the local authorities (Regierungspraesidium Tübingen (Germany), R3/19G). Nine female C57BL/6J mice (21 ± 1.7 g) and 13 female Sprague Dawley rats (307 ± 28.4 g) were obtained from Charles River Laboratories (Sulzfeld, Germany). Additionally, α -Syn(A30P) transgenic mice ($n = 14$, 12 females and 2 males, 100 ± 10 weeks old, 30 ± 3.4 g), which express human α -Syn with an A30P mutation under the Thy-1 promoter, and age-matched wild-type mice on the same C57BL/6J background ($n = 14$, 11 females and 3 males, 100 ± 11 weeks old, 32 ± 4.3 g), were bred in Hertie Institute for Clinical Brain Research (Tuebingen, Germany) and also kindly provided by Prof. Dr. Tiago Fleming Outeiro (University Medical Center Goettingen, Goettingen, Germany) (deviation from the original sample size calculation of $n = 16$ /group as $n = 2$ /group died during the PET scan). All animals were maintained in our vivarium on a 12:12 hour light-dark cycle and were kept at a temperature of 22°C with 40-60% humidity with free access to a standard diet and tap water.

Macaque experiments were conducted in compliance with all applicable sections of the Final Rules of the Animal Welfare Act regulations (Code of Federal Regulations, Title 9), the Public Health Service Policy on Humane Care and Use of Laboratory Animals from the Office of Laboratory Animal Welfare, and the Guide for the Care and Use of Laboratory Animals from the National Research Council (OLAW, current edition) (NRC, current edition). Adult (> 5–6 years

of age) male (n = 1, 6.0 kg, NHP 1) and female (n = 1, 6.4 kg, NHP 2) cynomolgus macaques (*Macaca fascicularis*) were maintained at Charles River Laboratories, Inc. (Mattawan, MI, USA, CRL Study No., 2579-100) on a 12:12 hour light-dark cycle. They were kept at temperatures of 18 to 29°C with 30–70% humidity with free access to a standard diet and tap water.

α -Syn fibril injection into the rat brain

Stereotactic surgeries were performed as previously described (14). Briefly, rats (n = 7) were intracranially injected with 4 μ L of α -Syn fibrils (30 μ M) using a stereotaxic injector (Stoelting, Wood Lane, IL, USA) (0.4 μ L every 60 seconds.) into the right striatum (medial-lateral = -3.4 mm, anterior-posterior = 0.0 mm, dorsoventral = -4.8 mm) according to the stereotaxic atlas of Paxinos and Watson (46). A contralateral injection of 4 μ L vehicle (50 mM Tris-buffer, 100 mM sodium chloride, 0.02% sodium azide, pH 7.0) served as negative control. PET imaging was performed either four days or between three to four days (for blocking study) post injection. Thioflavin S (ThS) staining on coronal 30 μ m cryosections of fibril-injected rats was performed as described in (14). Images were captured using a Leica DMI8 microscope and FITC filter settings (excitation 460 nm–500 nm; emission 512 nm–542 nm). Autoradiography of the cryosections was performed as described above, using 3 nM [³H]MODAG-005 and 3 μ M unlabeled MODAG-005 for blocking.

***In vivo* PET and MRI analysis in mice and rats**

PET imaging was performed as described previously on a dedicated small animal Inveon PET scanner (Siemens Healthcare, Knoxville (TN), USA) (14). Mice and rats were anaesthetized with 1.5-1.7% isoflurane evaporated in 100% oxygen at a flow rate of 0.8 L/min. Their body temperature was maintained at 37°C using a feedback temperature control unit. Five seconds after the start of the PET acquisition, mice for the pharmacokinetic study (n = 3) were injected intravenously (i.v.) with 14 ± 0.7 MBq of [¹¹C]MODAG-005 ($A_m = 37 \pm 9.2$ GBq/ μ mol at time of injection) and rats for the pharmacokinetic and fibril injection studies (four days post-injection) (n = 8) with 24 ± 3.0 MBq ($A_m = 41 \pm 6.8$ GBq/ μ mol at time of injection) produced by reductive methylation. For the blocking study in fibril-injected rats as well as the study in the α -Syn(A30P) transgenic mouse model, animals were injected i.v. with 27 ± 1.6 MBq ($A_m = 134 \pm 33.6$ GBq/ μ mol at time of injection) and 15 ± 0.9 MBq ($A_m = 175 \pm 82.4$ GBq/ μ mol at time of injection) of [¹¹C]MODAG-005, respectively, which was produced by direct methylation method A. For the blocking study in fibril-injected rats, two PET scans between three to four days after fibril injection were performed, which consisted of a baseline measurement with vehicle injection (20% PEG-400 (Carl Roth GmbH, Karlsruhe, Germany) and 80% of 20% aqueous sulfobutyl ether β -cyclodextrin sodium (CycloLab Ltd., Budapest, Hungary)) and a blocking measurement with the administration of anle138b (1 mg/kg dose in the vehicle) as a single intravenously bolus five minutes before tracer injection. For all experiments, dynamic PET data were acquired for 60 minutes, followed by a 13-minute transmission measurement with a cobalt-57 point source for attenuation correction.

For the pharmacokinetic study in mice, whole-body anatomical magnetic resonance images were acquired on a 7T small animal magnetic resonance imaging (MRI) scanner (Bruker BioSpin GmbH, Ettlingen, Germany). Animals were kept under 1.5% isoflurane anesthesia evaporated in 100% oxygen at a flow rate of 0.8 L/min. Signal transmission and readout were performed using a linearly polarized radiofrequency coil with an inner diameter of 72 mm (Bruker BioSpin GmbH, Ettlingen, Germany). A localizer sequence was used to position the mice in the centre of

the field-of-view (FoV). Anatomical images were acquired with a Turbo RARE T2 sequence (TR/TE 800 ms/35.1 ms, FoV 37.4 mm × 85.8 mm × 22.8 mm, Matrix 144 × 256 × 92).

Following the completion of imaging procedures, animals were sacrificed under CO₂ and perfused with cold PBS. Brains were extracted and frozen immediately either in 2-methylbutane cooled on dry ice (fibril-injected rats) or in TissueTek (mice).

OSEM3D was used as data reconstruction algorithm resulting in a final spatial resolution of 0.39 × 0.39 × 0.8 mm³. PET data for the pharmacokinetic and fibril injection studies were divided into 39 time frames (12×5 s, 6×10 s, 6×30 s, 5×60 s, and 10×300 s). For the blocking study in fibril-injected rats as well as the study in the α-Syn(A30P) transgenic mouse model, PET data were divided into either 45 frames (10 × 2 s, 8 × 5 s, 6 × 10 s, 6 × 30 s, 5 × 60 s, 10 × 300 s). Mouse PET scans were co-registered to the whole-body MRI scan. Based on the MRI anatomy, volumes of interest (VOIs) of the lung, liver, heart, brain, and kidneys were hand-drawn using PMOD software (version 3.2; PMOD Technologies, Zürich, Switzerland). The VOIs of different regions in the rat and mouse brain were extracted using the atlas provided by PMOD (47–49). TACs were extracted and converted to standardized uptake values (SUVs), calculated as in **equation (1)**:

$$SUV(t) = \frac{\text{radioactivity concentration } \left(\frac{kBq}{mL}\right)}{\frac{\text{injected dose } \left(\frac{kBq}{g}\right)}{\text{body weight}}}$$
 (1)

Additionally, the SUV ratio (SUVR) was calculated using the cerebellum or the left/sham-injected striatum as the reference region in the study in fibril-injected rats, and using the cortex as reference in the study in the α-Syn(A30P) mouse model. SUVR values were calculated with **equation (2)**:

$$SUVR = \frac{\text{radioactivity in target region}}{\text{radioactivity in reference region}}$$
 (2)

***In vivo* PET/MRI in non-human primates**

In vivo experiments in non-human primates (NHPs) were performed at Charles River Laboratories, Inc. (Mattawan, MI, USA) under the sponsorship of inviCRO LLC (Needham, MA, USA). Macaques were initially sedated by intramuscularly administering 5-10 mg/kg of ketamine and maintained under 2.0% isoflurane evaporated in 100% oxygen at a flow rate of 2 L/min. Body temperature was maintained at 38°C. Heart rate (BPM), body temperature, expired CO₂, respiration/min, pulse O₂%, % anesthetic gas, and oxygen (L/min) were monitored at approximately 15-minute intervals throughout the time course of the scans. The brains were placed in the center of the FoV in a Siemens microPET Focus 220 scanner (Siemens, Knoxville, TN) in a head-first supine orientation. Macaques received a three-minute intravenous injection of either 6 mL of vehicle control at baseline or 1 mg/kg dose of MODAG-005 beginning five minutes prior to the injection of 127 MBq (m) or 57 MBq (f) of [¹¹C]MODAG-005 (A_m at time of injection = 33 ± 7 GBq/μmol) produced by direct methylation method B. Dynamic PET data were acquired for 120 minutes and divided into 33 time frames (6 × 30 s, 3 × 60 s, 2 × 120 s, and 22 × 300 s). At least 14 days after the baseline scan, animals were re-scanned as above with 89 MBq (m) and 222 MBq (f) [¹¹C]MODAG-005 and in addition with a three-minute infusion of 1

mg/kg unlabeled MODAG-005 in the vehicle, five minutes before the start of the PET acquisition. The 1 mg/kg mass dose was chosen based on preclinical pharmacology and toxicology data demonstrating good tolerability and high expected occupancy. The cold compound was administered five minutes before [¹¹C]MODAG-005 to ensure adequate plasma and brain concentrations at tracer injection and accommodating the short half-life of ¹¹C. Arterial blood sampling for activity measurements in blood and plasma and metabolite analysis (identified in bold italic) through a right inguinal (external iliac) or left internal iliac artery vascular access port was performed during the PET acquisition at 0.25, 0.75, 1.25, 1.75, 2.25, 3.25, 4, **5, 10, 15, 30, 45, 60**, 90, and 120 minutes post tracer administration. Parent fraction data were modeled using a sigmoid function and the fitted curve was used to extrapolate the parent fraction to 120 min for kinetic modeling.

Following the PET acquisition, anatomical T₁-weighted images were acquired with a Philips Intera 1.5T MRI scanner using a focused-head 3D T₁FE (gradient spoiled) sequence. The PET data were rigidly co-registered to the MRI, and the MRI was normalized to the cynomolgus template; the combined transformations were used to map the PET volumes into cynomolgus template space to delineate VOIs. Ten VOIs were extracted from the brain using the brain atlas in PMOD 3.802. Time-activity curves (TACs) were extracted and converted to SUVs, calculated as in **equation (1)**.

Filtered back projection was used as data reconstruction algorithm at a 256 × 256 matrix. Volume of distribution (V_T) and K₁ values were estimated from a two-tissue-compartment model at baseline and after competition with MODAG-005. Model selection was based on visual inspection of the fits, the Akaike Information Criterion (AIC), and the ability to obtain stable V_T estimates with acceptable standard errors. For these data, the two-tissue compartment model consistently provided superior fits compared with simpler models and yielded stable V_T values across regions and scans.

***Ex vivo* metabolite analysis in plasma and brain**

Metabolite analysis in mice and rats was performed as described previously (14). Briefly, each anaesthetized mouse was injected with 204 ± 36.9 MBq of [¹¹C]MODAG-005 (A_m = 37 ± 11 GBq/μmol at time of injection), and each rat with 436 ± 2.7 MBq (A_m = 46 ± 0.8 GBq/μmol at time of injection) produced by reductive methylation using a tail vein catheter. Five or 15 minutes post tracer injection, blood plasma samples were collected by heart puncture and the perfused brain of the mouse or right hemisphere of the rat was homogenized in PBS. After sample preparation as described in (14), separation was achieved by reversed-phase radio-HPLC on a Luna C18(2) column (5 μm, 100 Å, 250 mm × 4.6 mm, Phenomenex, Aschaffenburg, Germany) with 0.1% trifluoroacetic acid in water/acetonitrile (70/30) and an isocratic flow of 1.5 mL/min. Data were decay corrected to the start-time-point of the first sample and analyzed as previously described using the peak analyzer function in Origin software (OriginLab Corporation, version 9.1G, Northampton, MA, USA) (14).

Plasma metabolite analysis in NHPs was performed from samples collected during the PET acquisition. An Agilent 1100 HPLC system, equipped with a coincidence detector for radioactivity and a diode array detector for UV that was set to 287 nm, was used. Plasma (500 μL) was diluted with a diluent solution (1.0 mL of 10 μg/mL cold MODAG-005 standard in water) and injected directly onto a Phenomenex Onyx monolithic column (10 × 100 mm), which was fitted with a 10×10 mm guard cartridge. The solvent A was 100 mM ammonium acetate, pH

8.0, and the solvent B was acetonitrile. The samples were analyzed using a gradient method. The parent compound HPLC retention time was identified by injection of 1 μL of [^{11}C]MODAG-005 mixed with 1.5 mL water containing 10 μg MODAG-005 and 5 μL DMSO. 50-200 μCi of a [^{11}C]MODAG-005 dose solution in a volume no greater than 0.25 mL was spiked into two 2.5 mL arterial blood samples, which were taken shortly before a dose injection, to measure *ex vivo* blood metabolism, and labelled as “Standard A”, and “Standard B”. Standard B was analyzed immediately post-processing from whole blood to plasma. Standard A was retained at room temperature and processed to plasma at the same time as the 120-minute post-injection sample. The *in vivo* metabolism of [^{11}C]MODAG-005 was analyzed from 3.5 mL arterial blood samples that were collected at 5, 15, 30, 45, and 60 minutes post injection. The whole blood samples were centrifuged at $1,300 \times g$ for six minutes at 4°C to separate plasma, of which 500 μL was injected into the metabolite profiling HPLC system for analyzing the radio-metabolites.

Data were analyzed as previously described (14) using the peak analyzer function in Origin software (OriginLab Corporation, version 9.1G, Northampton, MA, USA) with correction for radioactive decay within the respective run.

Human participants

Patients were referred to our experimental diagnostics unit for differential diagnostic evaluation in terms of imaging assessment of possible underlying αSYN pathology. The translational use of the [^{11}C]MODAG-05 was performed in a 74 year-old female patient diagnosed with clinically established overlap syndrome of MSA-P and MSA-C and subsequently in a male 52 year-old patient diagnosed with clinically established MSA-C according to the Movement Disorder Society Criteria for the Diagnosis of Multiple System Atrophy (19) supported by findings on MR imaging indicating advanced neurodegeneration. [^{11}C]MODAG-05 PET was also performed in a 50 year-old male patient with GBA-PD harboring a severe L444P mutation in the *GBA1* gene and in a 65 year-old asymptomatic participant, who aimed to rule out the presence of αSYN deposition and thereafter considered as healthy control (HC).

Clinical severity of patients with MSA was assessed using the Unified Multiple System Atrophy Rating Scale (UMSARS) (50), the severity of PD motor symptoms was assessed using the MDS-UPDRS part III (51), and global cognition was assessed using the Montréal Cognitive Assessment (MoCA) (52). The patient with MSA-C/-P-Overlap scored 22 points in the UMSARS part I (historical review of functional motor and non-motor impairment), 20 points in UMSARS part II (motor examination scale) and a UMSARS part IV score of 3 (global disability scale) as well as a MoCA total score of 24 of 30 points. The patient with MSA-C had a UMSARS part I score of 22, UMSARS part II score of 16 points, UMSARS part IV score of 2 and a MoCA total score of 26 of 30 points. The patient with GBA-PD had an MDS-UPDRS part III score (motor examination) of 44 points and a MoCA total score of 28 of 30 points.

Absence of Alzheimer’s co-pathology was determined in both MSA cases as well as in the GBA-PD case by cerebrospinal fluid (CSF) analysis of $\text{A}\beta_{1-42}$, $\text{A}\beta_{1-40}$, $\text{A}\beta_{1-42}/\text{A}\beta_{1-40}$ ratio, phospho181- and total Tau using a fully automated chemiluminescent enzyme immunoassay (CLEIA) with commercially available kits on the LUMIPULSE® G600II platform (Fujirebio Europe, Ghent, Belgium).

***In vivo* PET, SPECT and MRI in humans**

To confirm the underlying neurodegenerative Parkinson syndromes, dopamine transporter single-photon emission computed tomography (DAT SPECT) imaging (3 h p.i. of 185 MBq [¹²³I]FP-CIT; Discovery 670, GE Healthcare) was performed in patients with MSA-C/P and GBA-PD. The scans revealed a marked reduction in presynaptic dopamine transporter binding, indicative of pronounced nigrostriatal degeneration and in line with the clinical diagnosis of parkinsonian syndromes. PET imaging was performed on a highly sensitive Long Axial Field-of-View PET/computed tomography (CT) scanner (Biograph Vision Quadra, Siemens Healthineers) after intravenous bolus injection of [¹¹C]MODAG-005. Injected activity was 184 MBq for the patient with MSA-C, 49 MBq for the patient with MSA-C/P, 282 MBq for the patient with GBA-PD and 125 MBq for the HC. Dynamic PET data were acquired for 60 minutes and divided into 15 or 39 time frames (10 × 60 s, 5 × 600 s or 12×5 s, 6×10 s, 6×30 s, 5×60 s, and 10×300 s). OSEM3D was used as the data reconstruction algorithm and attenuation correction was applied based on the CT. Final reconstructed spatial resolution was 1.65 × 1.65 × 2.5 mm³ in x,y,z direction. In addition, a clinical 3T-MRI (Siemens Magnetom Prisma Fit) was performed at the same day which included (T1- and T2-weighted sequences). The PET data were co-registered to the respective MRI using PMOD software 4.2, and VOIs (right and left caudate, putamen, pons, midbrain, cerebellar white matter, frontal cortex and the occipital cortex) were drawn based on the anatomical information in the MR image using the PMOD Fusion Tool. TACs were extracted and converted to SUVs and normalized to the occipital cortex to generate SUVR values. The occipital cortex was chosen as reference region because it is among the cortical areas least affected by αSYN pathology across the synucleinopathy spectrum, particularly in early and moderate disease stages. Post-mortem studies in PD and MSA consistently indicate a caudo-rostral progression with predominant involvement of brainstem, limbic, and frontal-temporal regions, whereas the primary visual cortex is relatively spared until late stages.

In addition, the occipital cortex offers favorable properties for SUVR estimation: it is large, exhibits relatively homogeneous tracer kinetics, and is less susceptible to early atrophy compared to smaller candidate regions such as cerebellar cortex or brainstem nuclei, thereby reducing partial-volume effects. Alternative reference regions (e.g., cerebellar cortex, white matter) may be suitable in selected subgroups but are less robust across mixed cohorts, given that cerebellar involvement can occur in MSA-C and that white-matter pathology may vary across diseases. Parametric SUVR images were generated by dividing voxelwise SUV values from 30-60 min by the mean SUV of the occipital cortex. The 30-60 min interval was chosen because [¹¹C]MODAG-005 showed rapid uptake and fast washout of non-bound tracer, whereas regions with pathology displayed slower washout. Thus, image contrast and SUVR stability are maximal in this period. Peak SUVR values from each VOI were extracted from dynamic SUVR curves.

Supplementary Figures

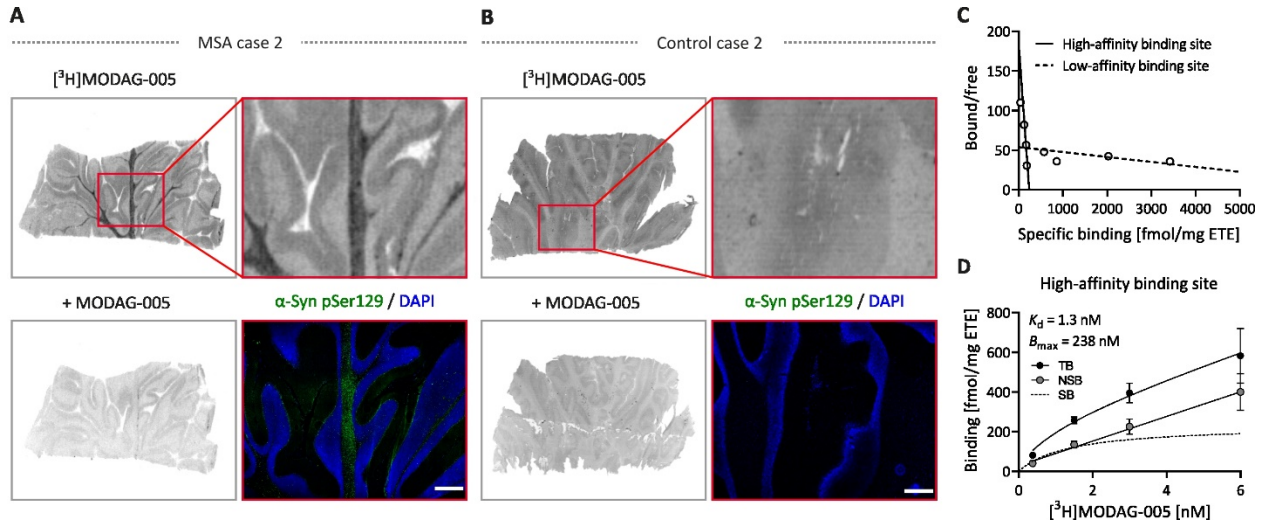


Fig. S1. $[^3\text{H}]\text{MODAG-005}$ exhibited binding in MSA case 2 brain tissues. Macroscopic autoradiography showing binding of $[^3\text{H}]\text{MODAG 005}$ to MSA case 2 white matter with verified c pathology (**A**) and control tissue case 2 with the absence of pathology (**B**). Pathology in tissue was verified by immunofluorescence of $\alpha\text{-Syn pSer129}$ (green) and DAPI (blue). Scale bars, 1 mm. All tissue sections were incubated in the presence of 3 nM $[^3\text{H}]\text{MODAG 005}$ and 3 μM MODAG 005 for blocking. (**C** and **D**) Saturation binding autoradiography in MSA case 2 as shown by Scatchard plot (**C**) and saturation binding curve (**D**) revealing the presence of high-affinity binding site ($K_d = 1.3 \text{ nM}$) after selegiline pre-blocking (3 μM for 1 hour) ($n = 1$, biological replicate, $N = 1$ technical replicate for each tracer concentration with repeated measurements in each sample). Abbreviations: $\alpha\text{-Syn}$, $\alpha\text{-synuclein}$; ETE, estimated tissue equivalent; MSA, multiple system atrophy; NSB, non-specific binding; SB, specific binding; TB, total binding.

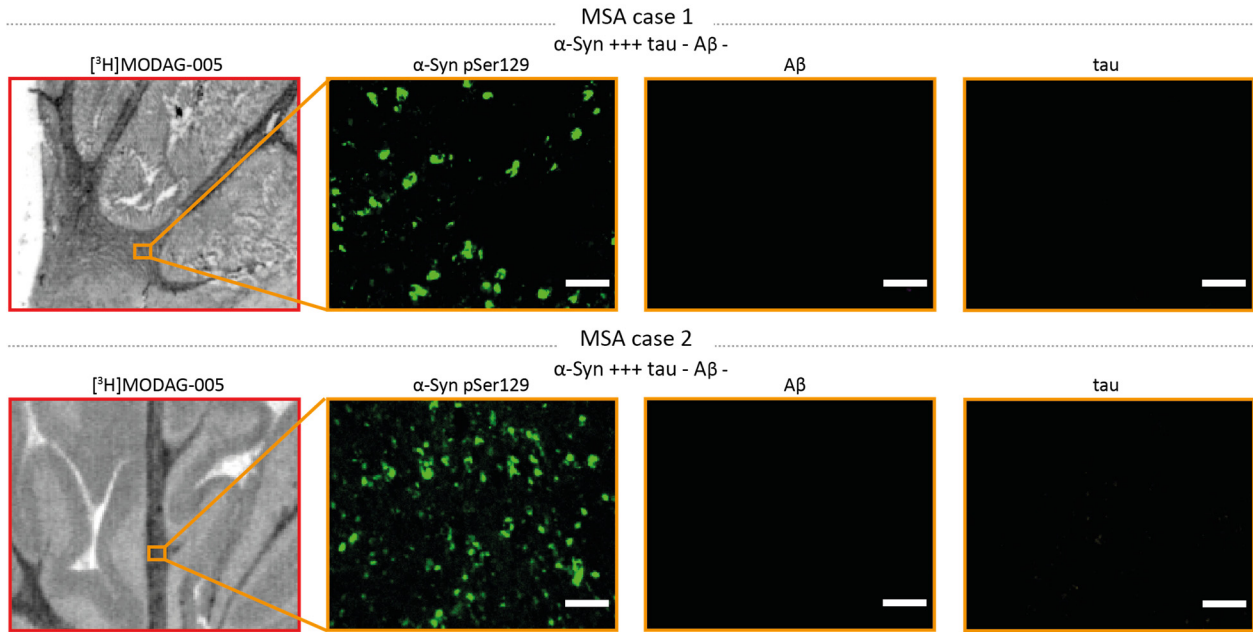


Fig. S2. α-Syn, Aβ and tau immunofluorescence microscopy on human MSA case 1 and 2 brain sections. The number of “+” symbols indicates an increasing degree of pathology; “-” symbolizes the absence of pathology. Scale bars, 50 μm. Abbreviations: Aβ, β-amyloid; α-Syn, α-synuclein; MSA, multiple system atrophy.

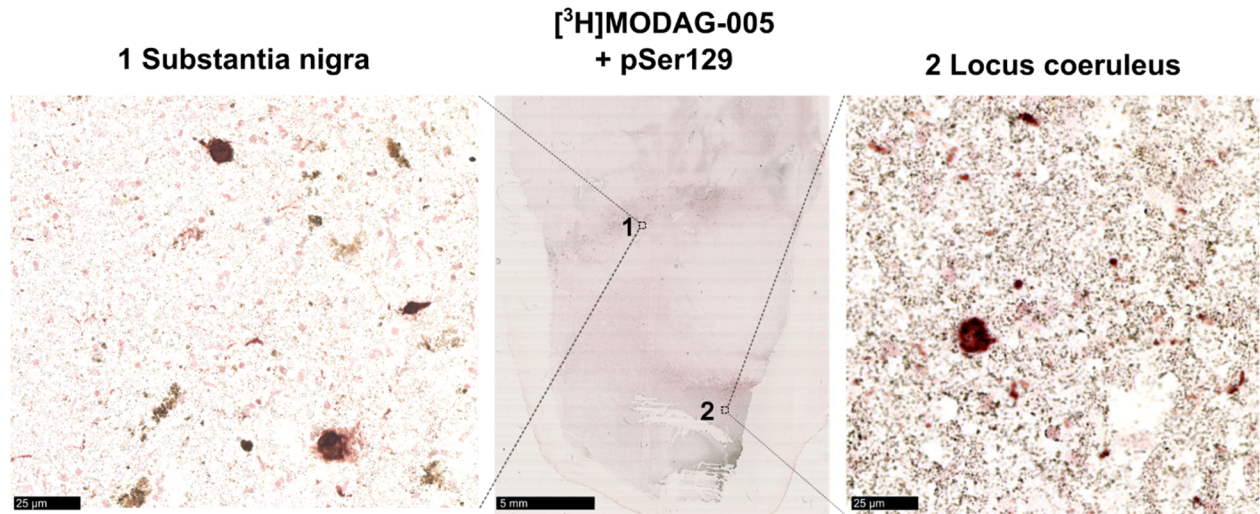


Fig. S3. [³H]MODAG-005 microautoradiography and subsequent immunohistochemistry on one brain slice of a PD case revealed tracer binding in the substantia nigra and locus coeruleus. High resolution (scale bar: right, left image: 25 μm, middle: 5 mm) of the substantia nigra (**1**) and locus coeruleus (**2**) showed Lewy pathology and accumulation of [³H]MODAG-005 (n = 1 biological replicate, N = 1 technical replicate).

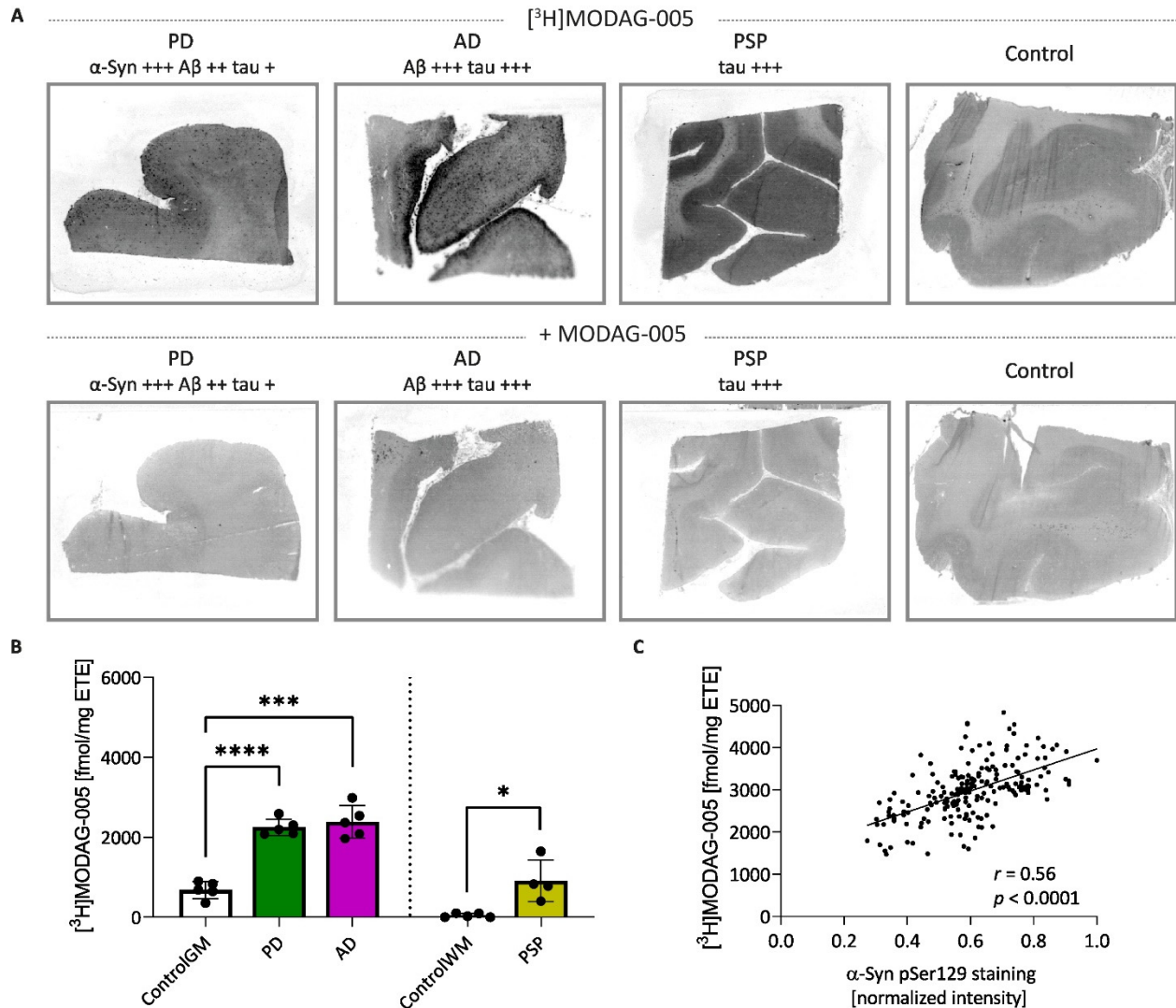


Fig. S4. [³H]MODAG-005 shows binding in post-mortem human brain tissues of PD, AD and PSP cases. (A) Autoradiography examining specific tracer binding in the frontal cortex of PD, AD, PSP, and control brain tissue. All tissue sections were incubated in the presence of 3 nM [³H]MODAG 005 and 3 μM MODAG 005 for blocking. (B) Quantitative analysis of autoradiography. Brown-Forsythe and Welch ANOVA with Dunnett's T3 multiple comparisons were used to compare ControlGM with PD ($p < 0.0001$) and AD ($p < 0.001$), and a two-way unpaired t-test with Welch's correction was used to compare ControlWM with PSP ($p = 0.045$). (C) Correlation analysis between [³H]MODAG-005 binding and α-Syn pSer129 immunofluorescence in the PD tissue ($r = 0.56$, $p < 0.0001$) (α-Syn pSer129 staining intensity was normalized by the maximum intensity). The number of “+” symbols indicate an increasing degree of pathology. Data in B are presented as mean ± SD. Data in B and C are from repeated measurements in each sample ($n = 1$ biological replicate, $N = 1$ technical replicate with repeated measurements in each sample). Abbreviations: AD, Alzheimer’s disease, α-Syn, α-synuclein; ETE, estimated tissue equivalent; GM, grey matter; PD, Parkinson’s disease; PSP, progressive supranuclear palsy; WM, white matter.

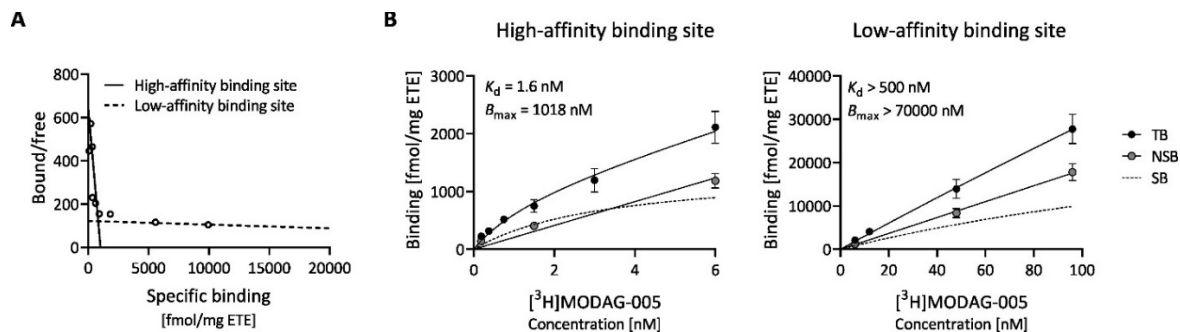


Fig. S5. $[\text{}^3\text{H}]\text{MODAG-005}$ showed binding in AD brain tissue. Saturation binding autoradiography in AD brain tissue ($n = 1$, repeated measurements in each sample). **(A)** Scatchard plot revealing the presence of two binding sites in AD tissue. **(B)** Saturation binding curves of high-affinity and low-affinity binding sites. Data in **B** are the mean \pm SD. $n = 1$ biological replicate, $N = 1$ technical replicate for each tracer concentration with repeated measurements in each sample. Abbreviations: ETE, estimated tissue equivalent; NSB, non-specific binding; SB, specific binding; TB, total binding.

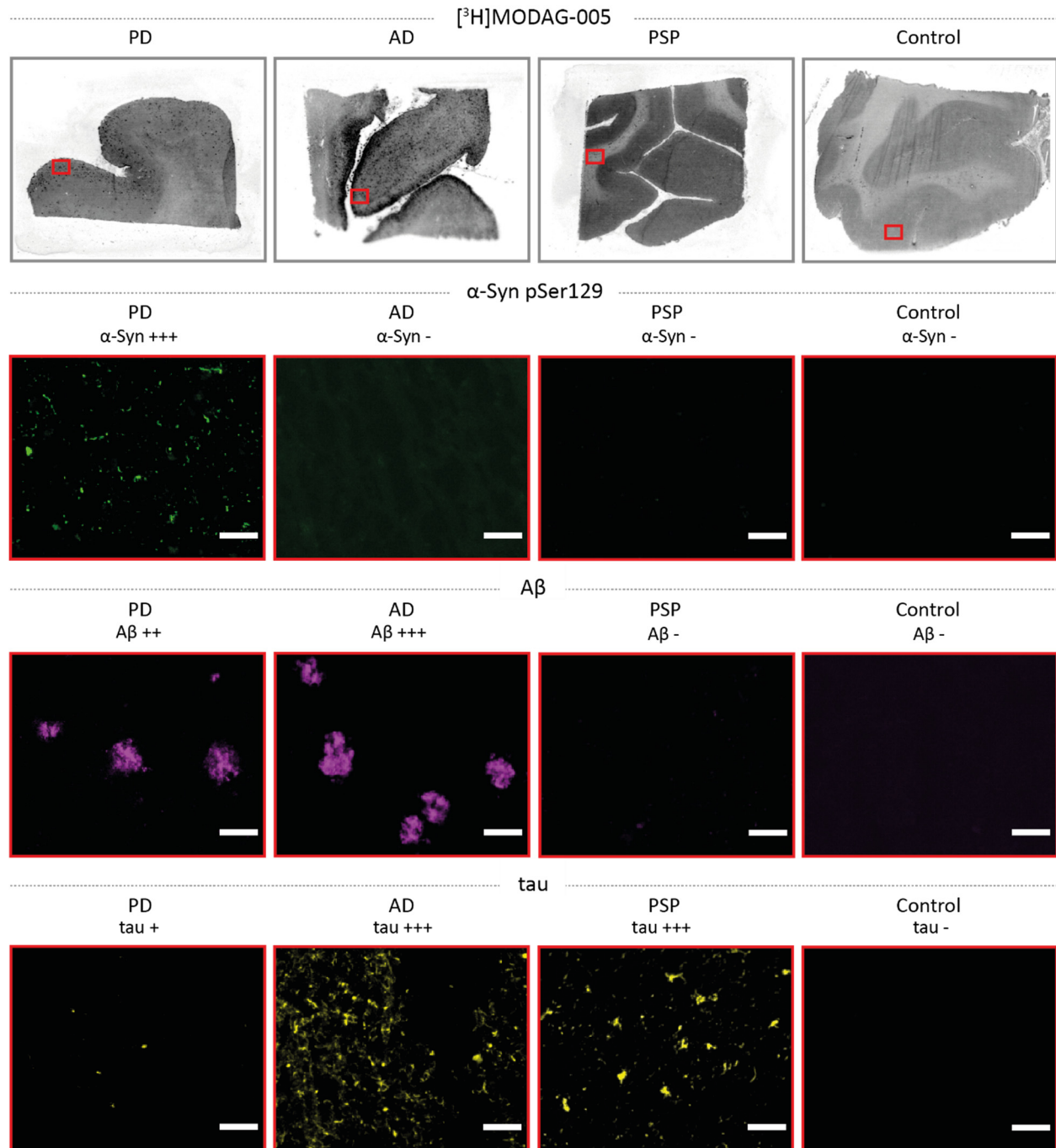


Fig. S6. α-Syn, Aβ and tau pathology on human brain sections was confirmed through immunofluorescence microscopy. Verification of the pathology in brain tissues using immunofluorescence of α-Syn pSer129 (green), Aβ₁₋₄₂ (magenta) and phosphorylated tau (yellow). The number of “+” symbols indicates an increasing degree of pathology; “-” symbolizes the absence of pathology. Scale bars, 50 μm. Abbreviations: AD, Alzheimer’s disease; Aβ, β-amyloid; α-Syn, α-synuclein; PD, Parkinson’s disease; PSP, progressive supranuclear palsy.

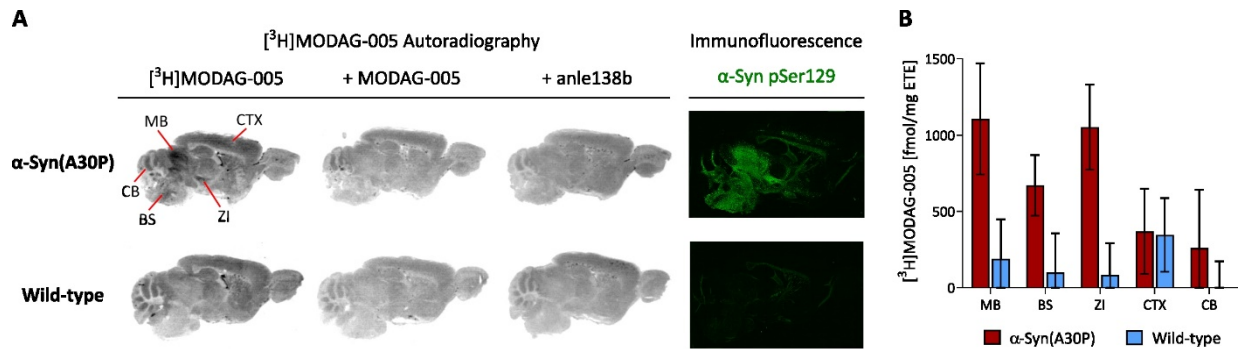


Fig. S7: [³H]MODAG-005 exhibited binding and anle138b target engagement in the α-Syn(A30P) mouse model of PD. Autoradiography was performed with 3 nM [³H]MODAG-005 and 3 μM unlabeled MODAG-005 or anle138b for blocking. **(A)** [³H]MODAG-005 total binding, self-blocking and anle138b blocking in brain sections of an α-Syn(A30P) mouse and an age-matched wild-type mouse (72 weeks old). α-Syn pSer129 immunofluorescence (green) validation of pathology distribution. **(B)** Quantitative analysis of autoradiography. Data are the mean ± SD obtained from repeated measurements in technical replicates (three for [³H]MODAG-005 and two for [³H]MODAG-005 + MODAG-005). in an α-Syn(A30P) mouse and a wild-type mouse (n = 1 biological replicate). No statistical test was performed. Abbreviations: α-Syn, α-synuclein; BS, brainstem; CB, cerebellum; CTX, cortex; ETE, estimated tissue equivalent; MB, midbrain; ZI, *zona incerta*.

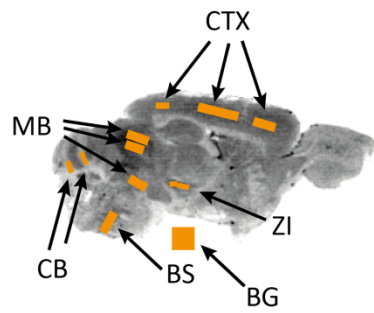


Fig. S8. Placement of regions of interest for [³H]MODAG-005 quantification in the α -Syn(A30P) mouse model of PD. Abbreviations: BG, background; BS, brainstem; CB, cerebellum; CTX, cortex; MB, midbrain; ROI, region of interest; ZI, *zona incerta*.

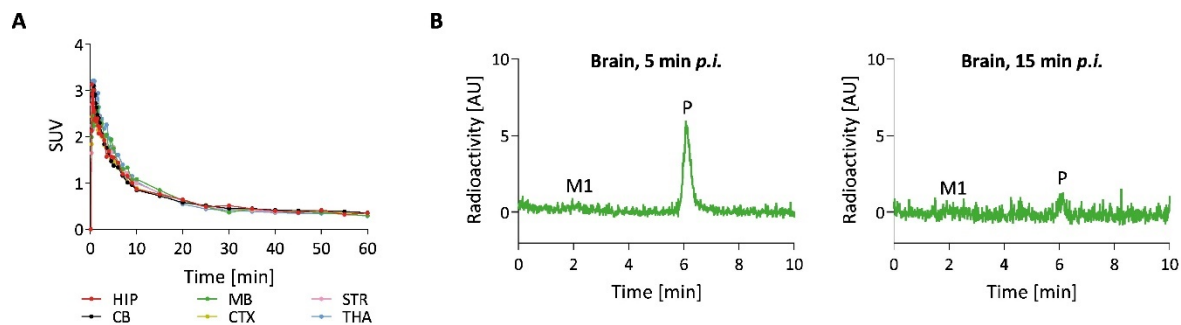


Fig. S9. Pharmacokinetic and metabolic profile of $[^{11}\text{C}]\text{MODAG-005}$ in the rat brain indicated the tracer suitability for brain imaging. (A) $[^{11}\text{C}]\text{MODAG-005}$ brain TACs in rat ($n = 1$ biological replicate, $N = 1$ technical replicate). (B) Radio-metabolite analysis revealing the presence of one metabolite present in the brain ($n = 1$ per time point, $N = 1$ technical replicate). Abbreviations: AU, arbitrary units; CB, cerebellum; CTX, cortex; HIP, hippocampus; MB, midbrain; M1, metabolite 1; P, parent compound; p.i., post injection; STR, striatum; SUV, standardized uptake value; THA, thalamus.

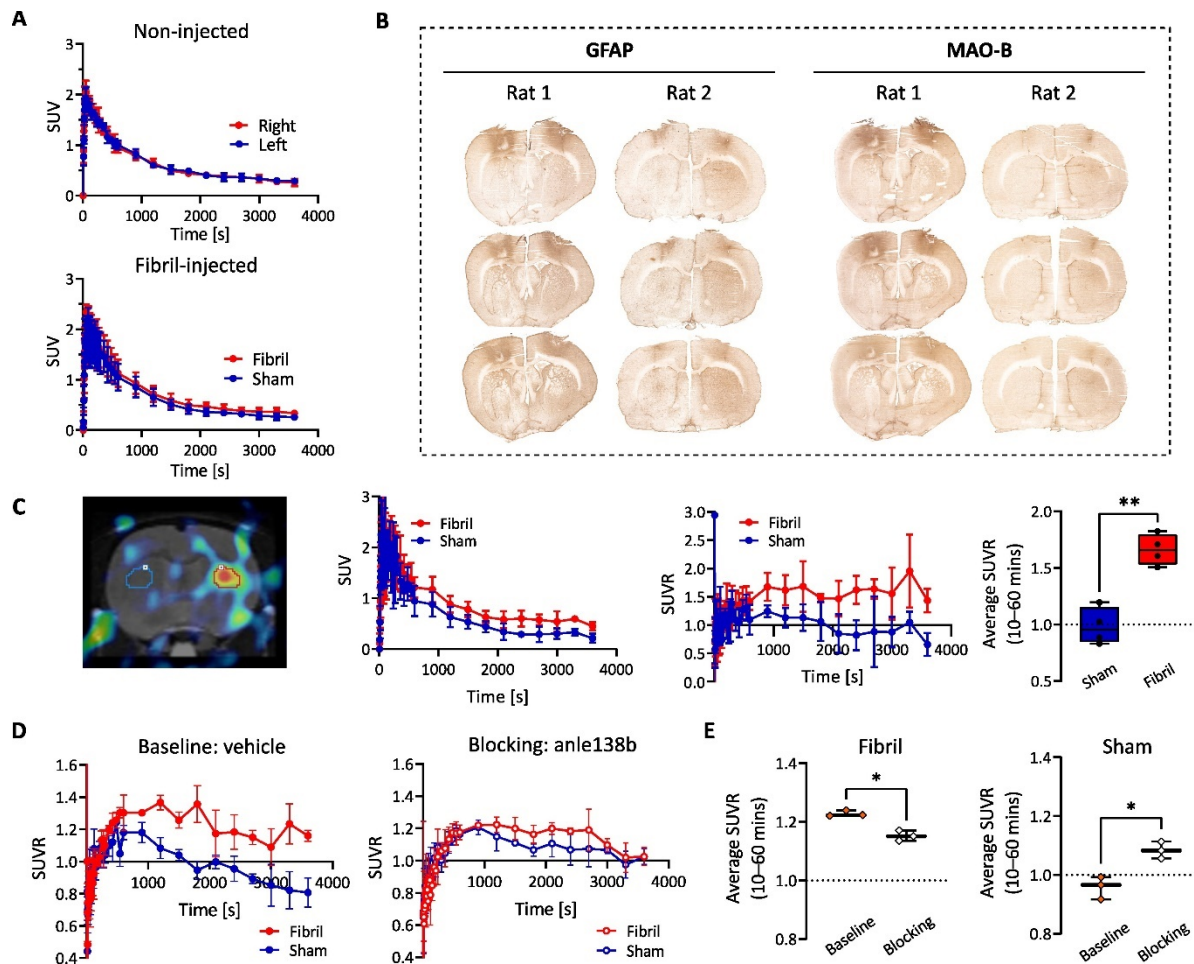


Fig. S10. PET analysis of [¹¹C]MODAG-005 and immunohistochemistry assessment of GFAP and MAO-B expression in fibril-injected rats further indicated specific binding to α -Syn. (A) TACs in the striatum of non-injected rats ($n = 3$) and fibril-injected rats ($n = 4$). (B) Immunohistochemistry of GFAP and MAO-B in brain slices of fibril-injected rats ($n = 2$). (C) PET analysis using VOI based on isocontour automatic detection set to 70% - an example PET/MR image with VOI (left) which were created surrounding the hotspot in the fibril-injected striatum (red) and subsequently mirror-reflected into the contralateral, sham-injected striatum (blue). TACs and time-SUVR curves (middle) as well as average SUVR (right) with the cerebellum as the reference. (D and E) Time-SUVR curves and average SUVR of fibril-injected rats which underwent a baseline scan with vehicle administration and a blocking scan with anle138b administration, using cerebellum as the reference region ($n = 3$). Average SUVR was decreased by anle138b blocking ($p = 0.038$) in the fibril-injected striatum, but increased in the sham-injected striatum ($p = 0.019$). Data are the mean \pm SD. $N = 1$ technical replicate for all experiments. An unpaired two-tailed t-test was used in C and E. Abbreviations: GFAP, glial fibrillary acid protein; MAO-B, monoamine oxidase B; SUV, standardized uptake value; SUVR, standardized uptake value ratio; VOI, volume of interest.

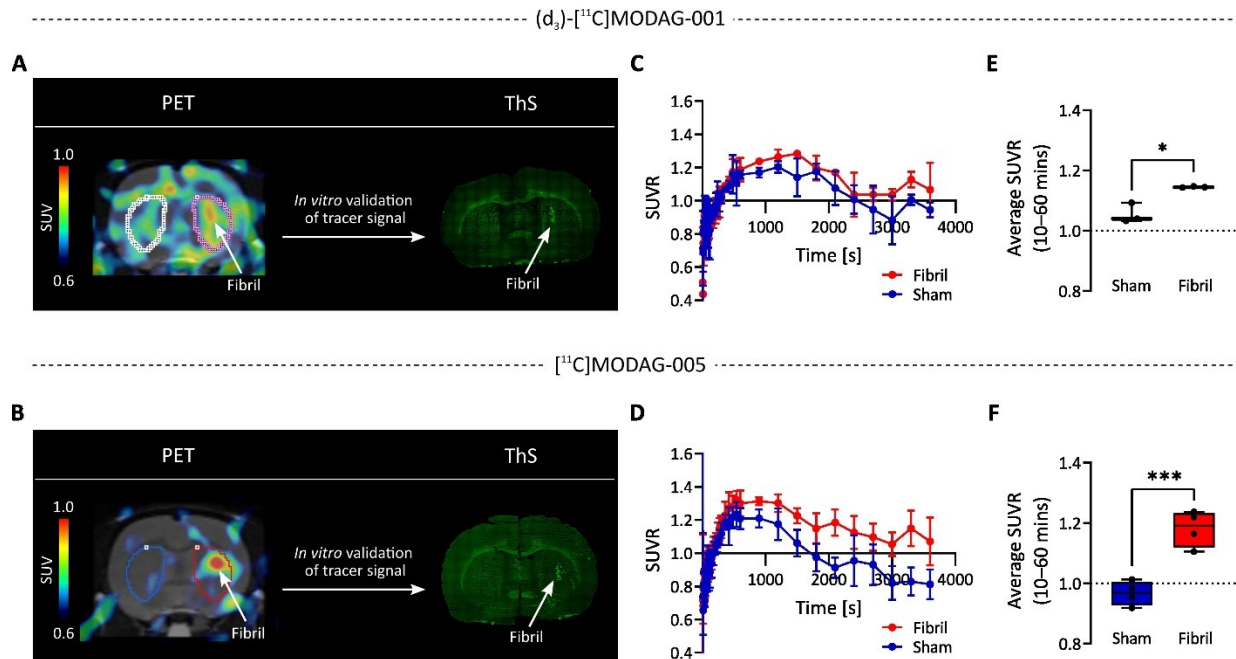


Fig. S11. [¹¹C]MODAG-005 exhibited an improved target-to-background ratio compared to (d₃)-[¹¹C]MODAG-001 *in vivo*. (A) (d₃)-[¹¹C]MODAG-001 and (B) [¹¹C]MODAG-005 PET images (sum of 2.5 to 60 min) of exemplary α -Syn fibril-injected rats four days post injection into the brain. (C and D) Time-SUVR curves and (E and F) average SUVR showing an improved target-to-background ratio for [¹¹C]MODAG-005 ($n = 4$, $p = 0.0003$) compared to (d₃)-[¹¹C]MODAG-001 ($n = 3$, $p = 0.045$). $N=1$ technical replicate for all experiments. Two-tailed paired t-tests were performed. Data are the mean \pm SD. Abbreviations: α -Syn, α -synuclein; PET, positron emission tomography; SUV, standardized uptake value; SUVR, standardized uptake value ratio; ThS, thioflavin S.

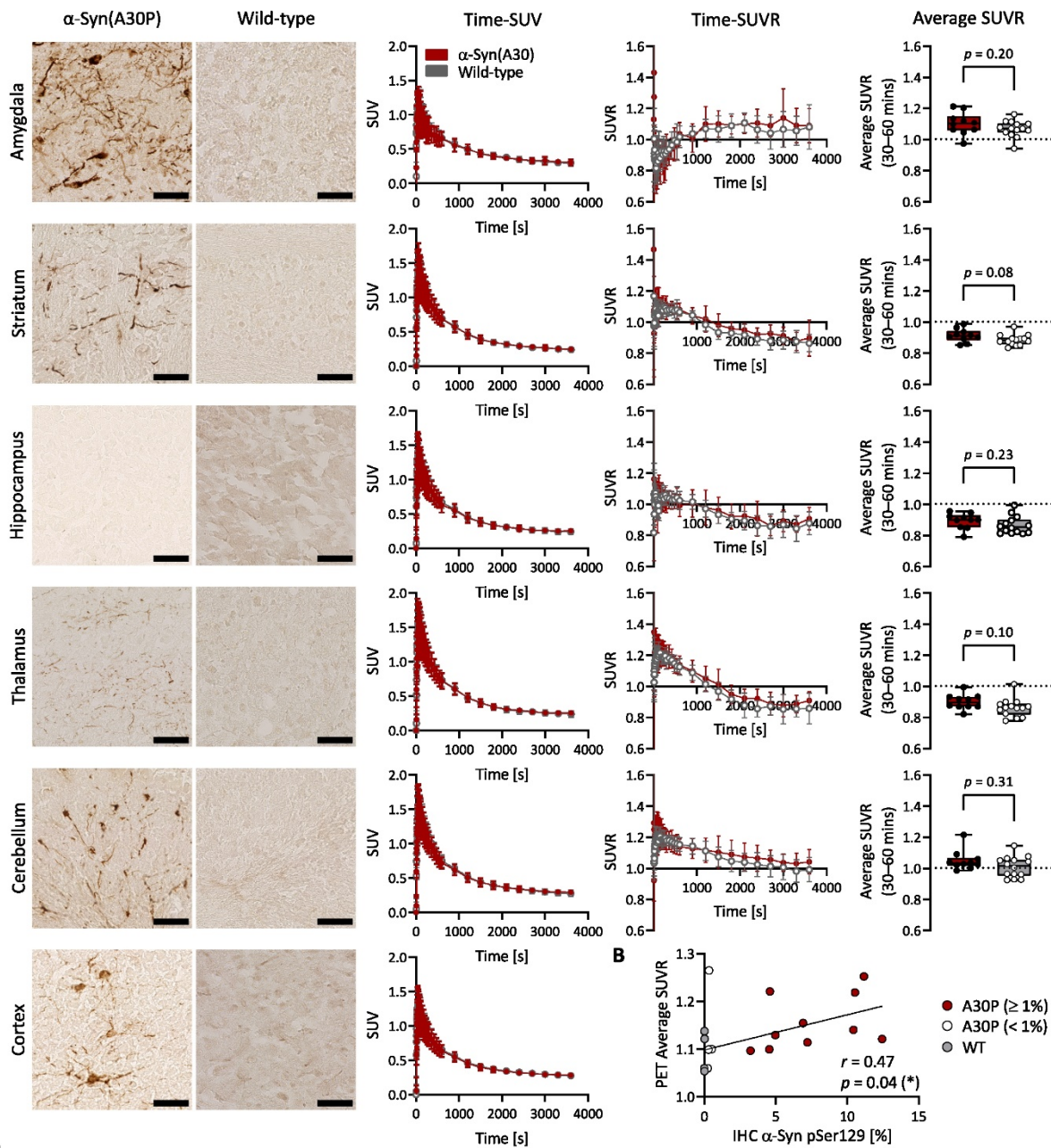
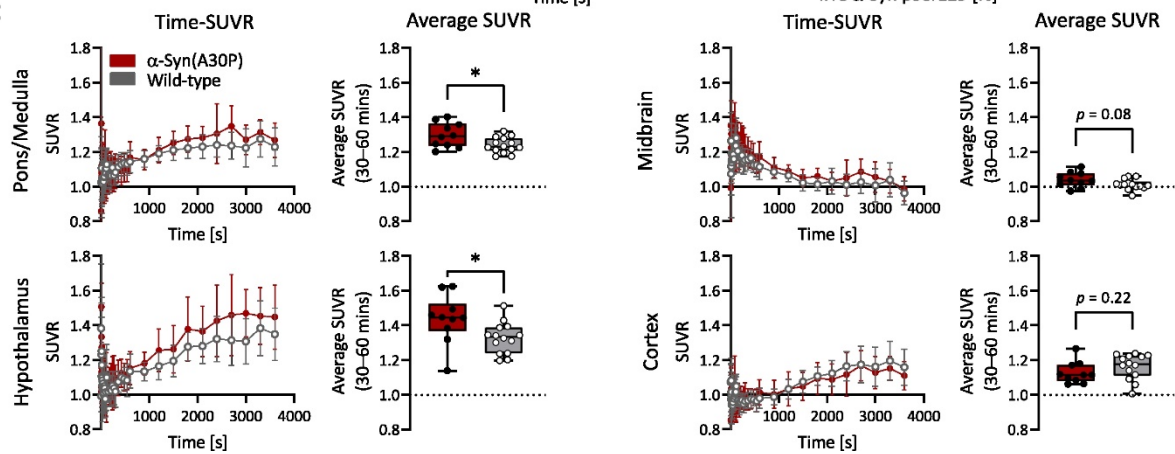
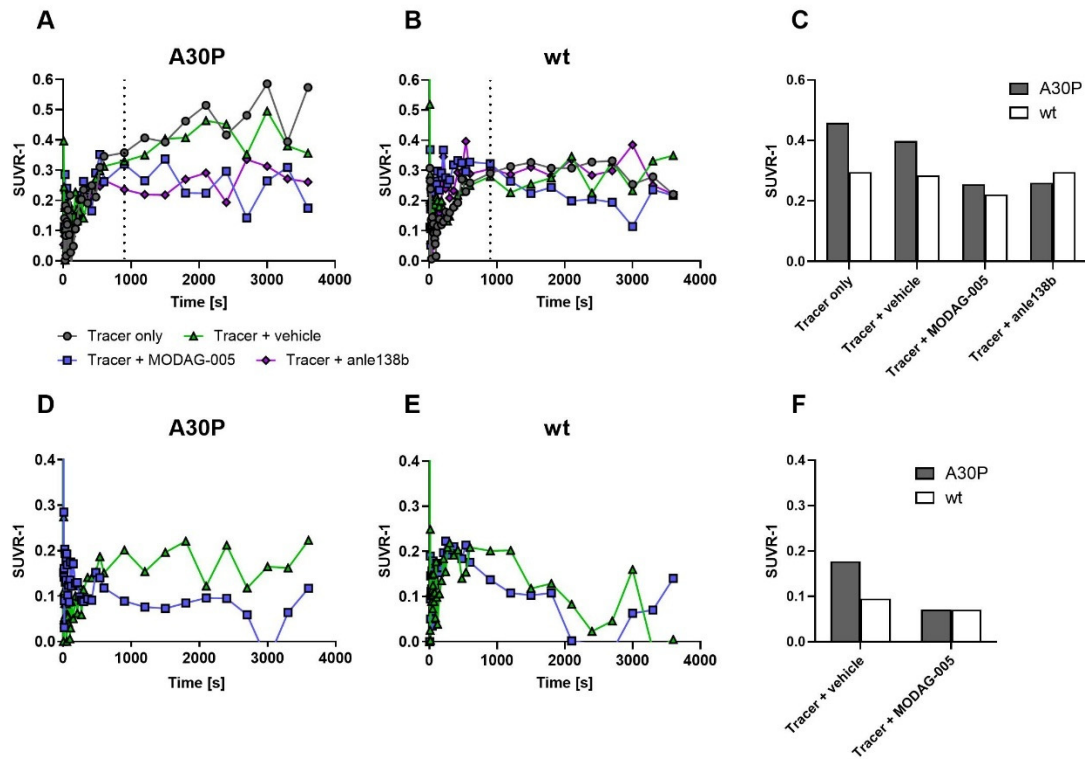
A α -Syn pSer129 $[^{13}\text{C}]\text{MODAG-005}$ PET**C**

Fig. S12. [¹¹C]MODAG-005 PET in the α -Syn(A30P) transgenic mouse model and immunohistochemical validation showed tracer binding in brain regions with high pathology load. (A) α -Syn pSer129 immunohistochemistry, PET time-SUV, time-SUVR and average SUVR comparison between α -Syn(A30P) mice and wild-type mice in various brain regions. Scale bar, 50 μ m. (B) Correlation analysis of the percentage positive α -Syn pSer129 immunohistochemistry and PET average SUVR in the pons/medulla of α -Syn(A30P) and wild-type mice ($r = 0.47$, $p = 0.04$). Individual heterogeneity of pathology load ranging from 0.2% to 12.4% was observed (see x-axis). α -Syn(A30P) mice with less than 1% positive staining signal were excluded from the main PET analysis shown in Fig. 5 and Fig. S12A/C. (C) [¹¹C]MODAG-005 PET time-SUVR curves and average SUVR comparison between α -Syn(A30P) mice and wild-type mice using the hippocampus as the reference region showing elevated binding in pons/medulla ($p = 0.02$) and hypothalamus ($p = 0.03$). In A and C, data points in time-SUV and time-SUVR curves are the mean \pm SD ($n = 10$ for α -Syn(A30P) mice and $n = 14$ for wild-type mice). An unpaired two-tailed t-test was performed to compare the average SUVR values for all brain regions except in the cerebellum where Mann-Whitney test was performed. In B, data points are presented as the mean value of individual animals in immunohistochemistry pathology quantification from all A30P α -Syn mice ($n = 14$, 6–10 tissue sections per animal) and randomly selected wild-type mice ($n = 5$, 2 tissue sections per animal). $N = 1$ technical replicate for all experiments. Abbreviations: A30P, α -Syn(A30P) mice; α -Syn, α -synuclein; IHC, immunohistochemistry; PET, positron emission tomography; SUV, standardized uptake value; SUVR, standardized uptake value ratio; WT, wild-type mice.



++

++

Fig. S13: Blocking effect was observed in [¹¹C]MODAG-005 baseline and blocking experiments in the α -Syn(A30P) mouse model. (A-C) SUVR-1 TACs in α -Syn(A30P) and wildtype (wt) mice and summed values from 900-3600s at baseline and after vehicle, MODAG-005 and anle138b injection at 900s after tracer injection (n = 1, dashed line). A blocking effect was observed in the α -Syn(A30P) mouse. (D-F) shows TACs and summed values at baseline and after co-injection of non-radioactive MODAG-005, showing a prolonged retention of [¹¹C]MODAG-005 in the α -Syn(A30P) mouse compared to the wildtype mouse (n = 1). N = 1 technical replicate for all experiments. The cortex was used as reference region. SUVR, standardized uptake value ratio.

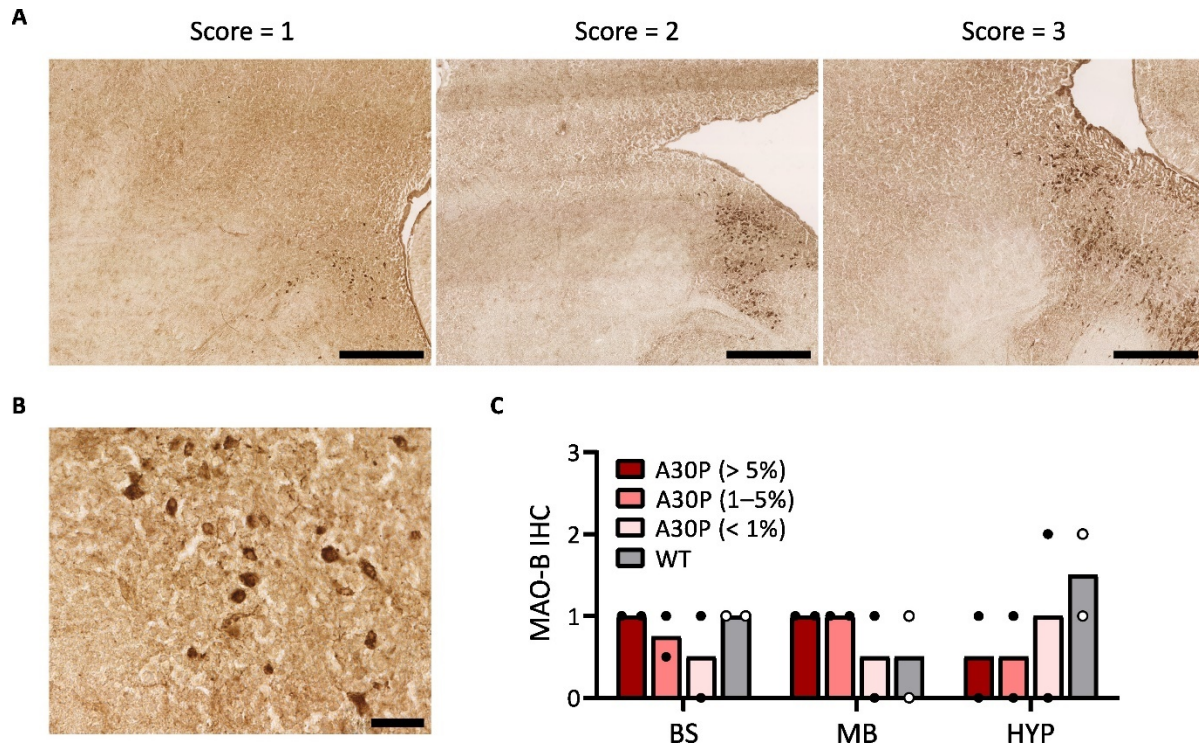


Fig. S14. Immunohistochemistry analysis showed no difference in the amount of MAO-B expression in α -Syn(A30P) and wild-type mouse brain sections. α -Syn(A30P) mice were assessed in three groups based on their α -Syn pSer129 pathology load as determined previously (A30P > 5%, A30P = 1–5%, A30P < 1%). Qualitative scoring (score 0–3, where 0 indicates no staining and 3 indicates relatively abundant staining) was performed for the brainstem, midbrain and hypothalamus. **(A)** Example of MAO-B immunohistochemistry images with their respective given score. Scale bar, 500 μ m. **(B)** Example of MAO-B immunohistochemistry showing a staining diameter of approximately 10 μ m. Scale bar, 50 μ m. **(C)** Immunohistochemistry analysis by qualitative scoring (n = 2 per animal group, 4 tissue sections per animal). Abbreviations: A30P, α -Syn(A30P) mice; BS, brainstem; HYP, hypothalamus; IHC, immunohistochemistry; MB, midbrain; WT, wild-type.

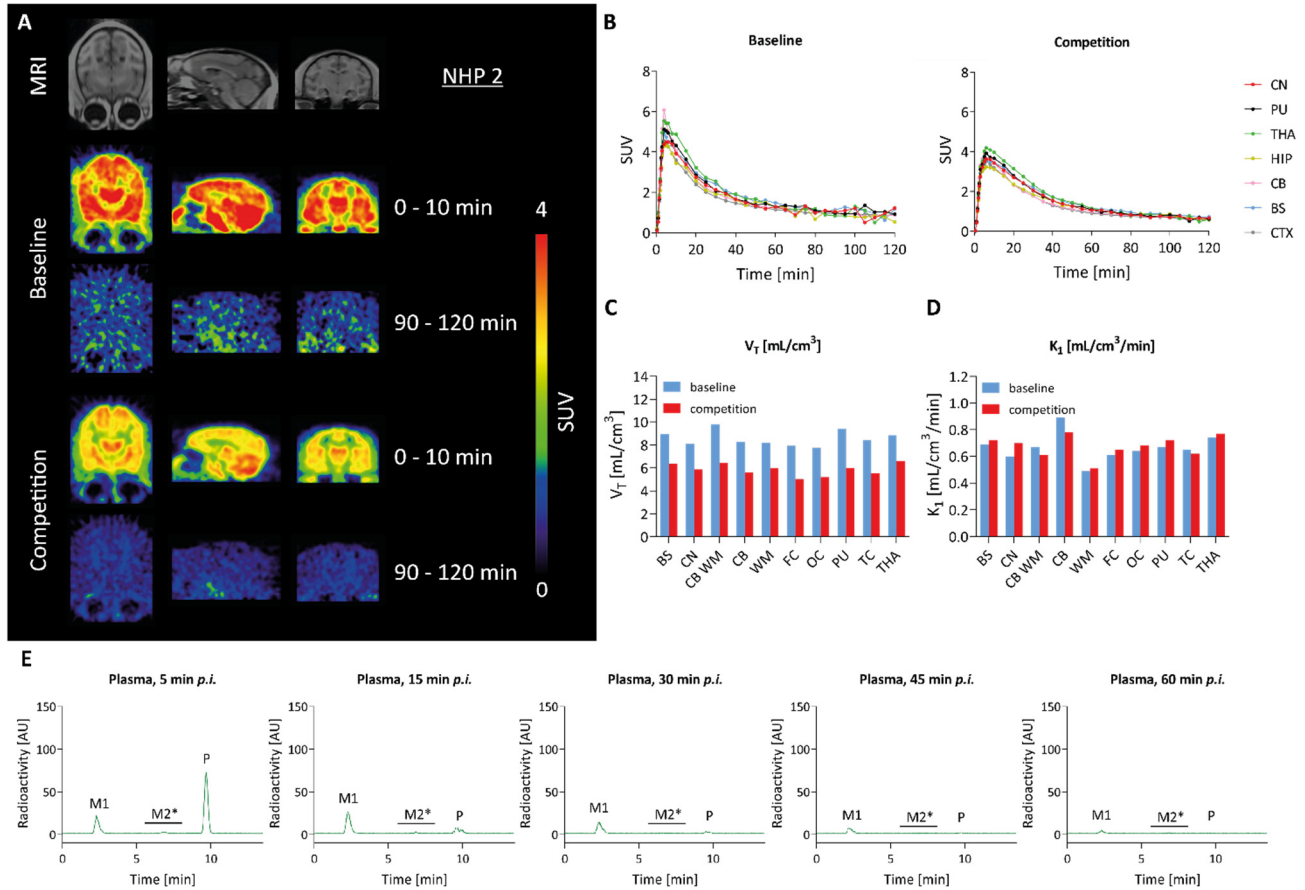


Fig. S15. *In vivo* characterization of $[^{11}\text{C}]\text{MODAG-005}$ in non-human primates (NHP 2) indicated favorable tracer attributes for brain imaging. (A) MRI and $[^{11}\text{C}]\text{MODAG-005}$ PET images (SUV) at baseline and after pre-injection of unlabeled MODAG-005. (B) TACs of different brain regions showing high brain uptake with peak SUVs of 6.1 (baseline) and 4.2 (competition) followed by a fast clearance from the brain. (C and D) Volume of distribution (V_T) and K_1 values estimated from a two-tissue-compartment model at baseline and after competition with MODAG-005. (E) Radio-metabolite analysis of plasma samples at 5, 15, 30, 45 and 60 minutes post tracer injection ($n = 2$ biological replicates, $N = 1$ technical replicate, see Fig. 6 for results from the first NHP).. Abbreviations: AU, arbitrary units; BS, brainstem; CB, cerebellum; CB WM, cerebellar white matter; CN, caudate nucleus; CTX, cortex; WM, white matter; FC, frontal cortex; HIP, hippocampus; MRI, magnetic resonance imaging; M1, metabolite 1; M2*, metabolite 2*; OC, occipital cortex; P, parent compound; PET, positron emission tomography; p.i., post injection; PU, putamen; STR, striatum; SUV, standardized uptake value; TACs, time-activity curves; TC, temporal cortex; 2-TCM, two tissue compartment model; THA, thalamus.

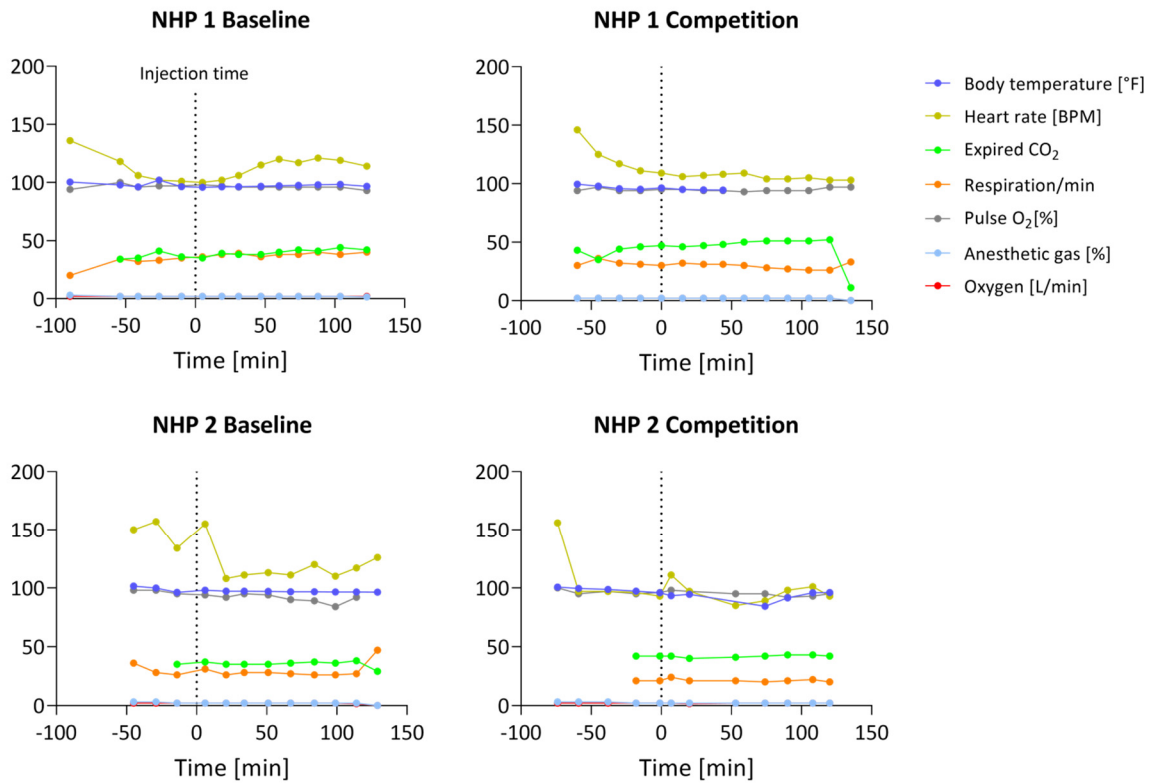


Fig. S16. Macaque vitals. Monitoring of heart rate (BPM), body temperature (°F), expired CO₂, respiration/min, pulse O₂ (%), anesthetic gas (%), and oxygen (L/min) throughout the NHP PET scans (n = 2 biological replicates, N = 1 technical replicates). Time is shown relative to tracer injection.

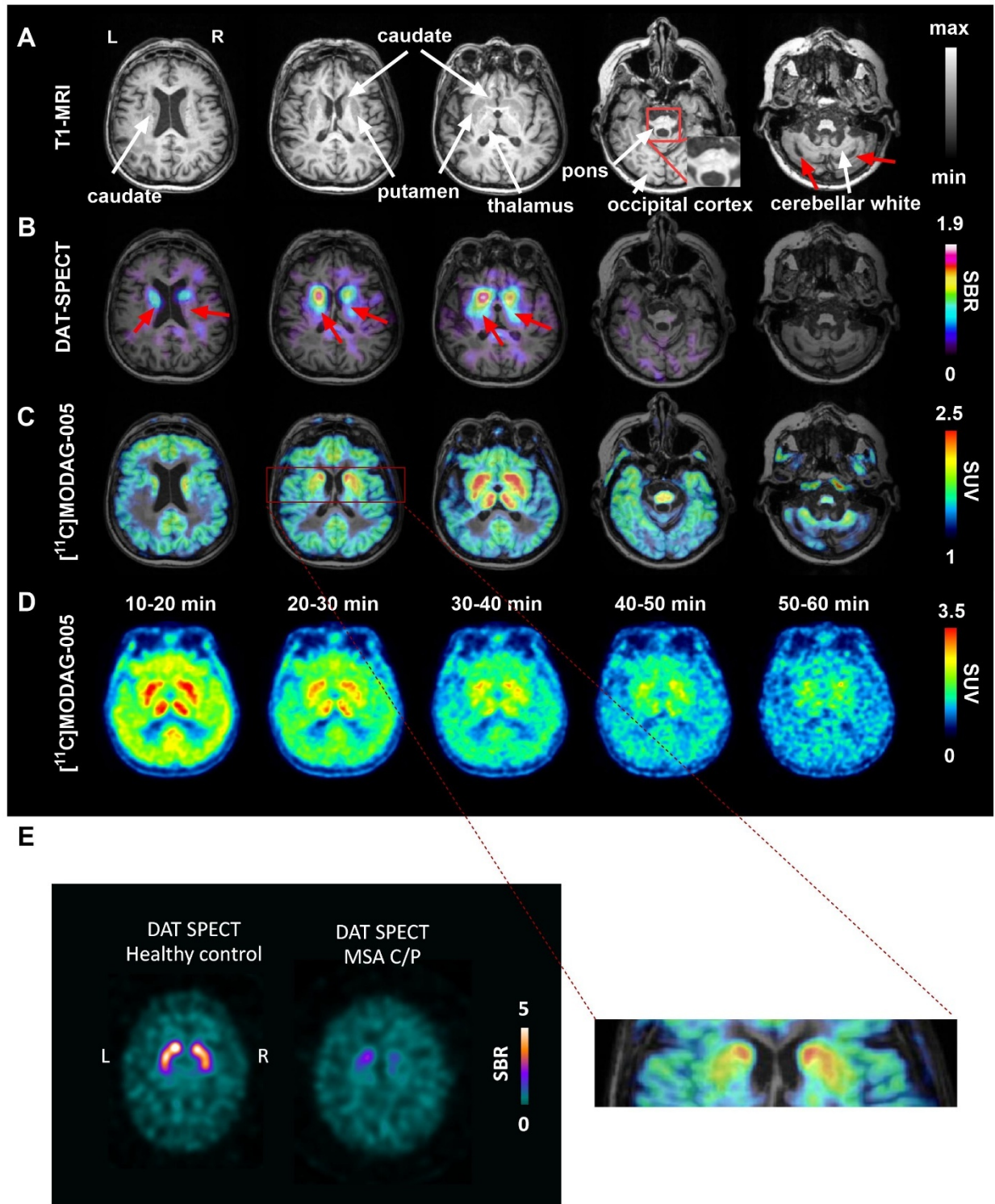


Fig. S17: [^{11}C]MODAG-005 first-in-human PET in a patient with MSA-C/P/ was supported by MR and dopamine transporter SPECT scans. (A) Transversal MR scans of a patient clinically diagnosed with an overlap syndrome of MSA-P and MSA-C (n = 1, N = 1), highlighting advanced cerebellar and pontine atrophy with the “Hot Cross Bun” sign reflecting degeneration of pontocerebellar tracts (indicated by red arrows and zoomed insert). White arrows

indicate anatomical regions which showed pronounced [¹¹C]MODAG-005 uptake. **(B)** Dopamine transporter (DAT) SPECT images, revealing presynaptic dopaminergic degeneration in the bilateral striatum (caudate and putamen (CPu)) with a more pronounced effect on the right side. **(C)** [¹¹C]MODAG-005 PET images (sum of 20-60 min) illustrating elevated binding in the bilateral striatum. Additionally, high binding is noted in the thalamus, pons and cerebellar white matter – regions associated with expected α -Syn pathology. **(D)** The pharmacokinetic profile of [¹¹C]MODAG-005 in a representative slice. Conversely, regions expected to exhibit α -Syn pathology showed prolonged tracer retention. **(E)** Lateralization of the pathology is shown in DAT SPECT images in comparison to a healthy control as well as in the CPu of the patient with MSA-C/P (zoom, n = 1, N = 1). MRI, magnetic resonance imaging; PET, positron emission tomography; SBR, specific binding ratio; SUVbw, standardized uptake value (normalized to body weight); SPECT, single photon emission computer tomography; DAT, dopamine transporter.

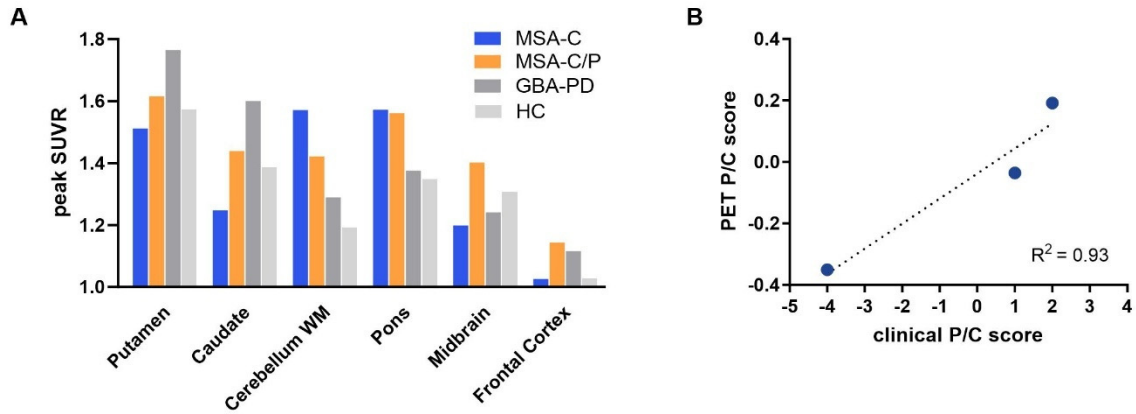


Fig. S18: [¹¹C]MODAG-005 SUVR values of patients with MSA-C, MSA-C/P, PD-GBA, and HC suggested tracer binding consistent with the expected relative distribution of α SYN pathology. (A) Comparison of regional peak SUVR values revealed a characteristic pattern of tracer binding in brain regions with expected α -Syn pathology (n = 1 for each case, N = 1). (B) Correlation of the peak PET ratio of signal intensity (peak SUVR) in putamen, caudate and midbrain versus pons and cerebellar white matter with the clinical score of parkinsonian versus cerebellar phenotype (P/C) indicates that tracer signal corresponds to the expected relative distribution of α -Syn pathology ($r = 0.93$). SUVR, standardized uptake value ratio.

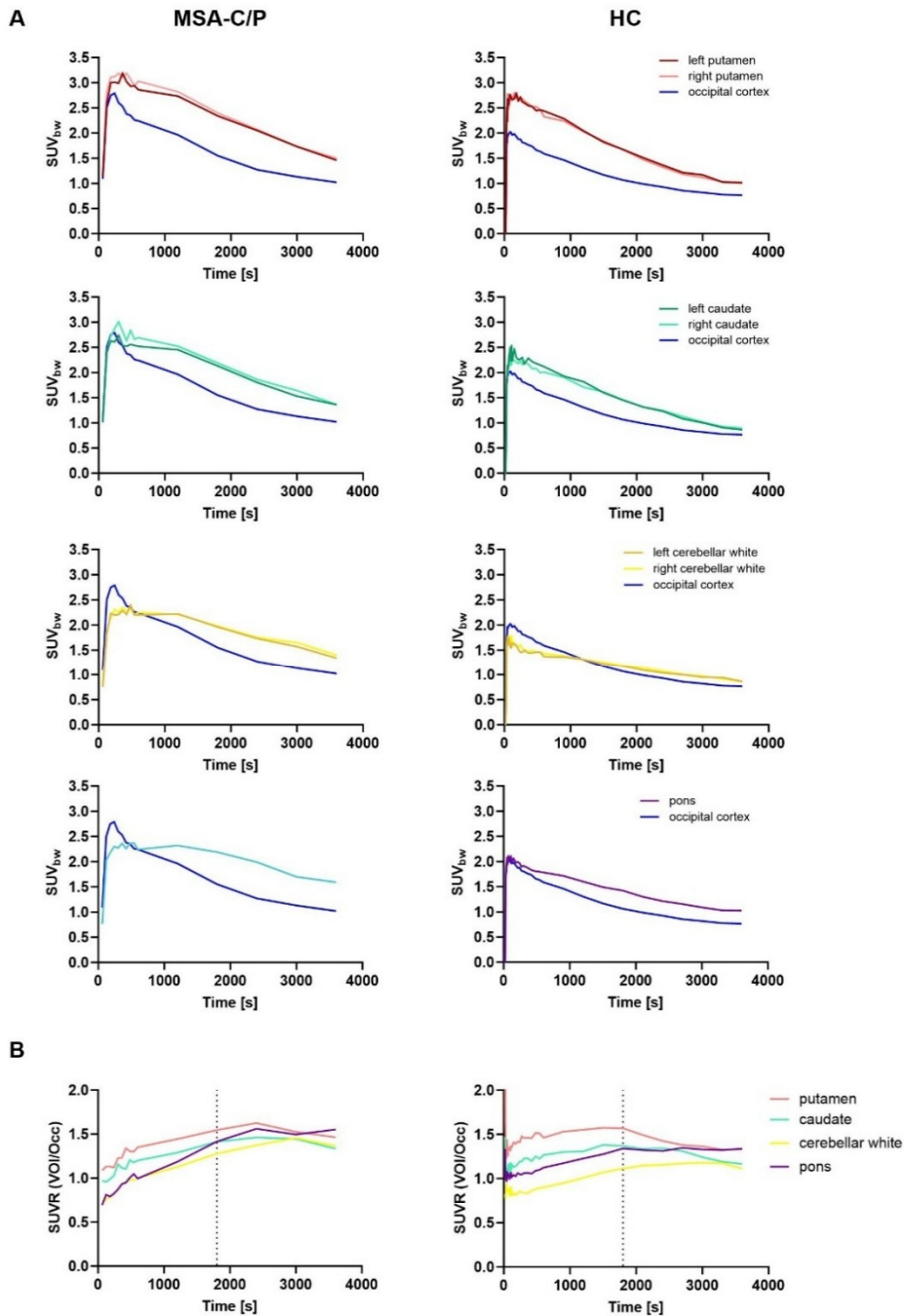


Fig. S19. Time-activity curves and time-SUVR curves of selected brain regions revealed prolonged tracer retention in brain regions with expected α SYN pathology. (A) SUV TACs ($n = 1$, $N = 1$) demonstrated rapid brain uptake (peak SUV: 2-2.8) and moderately fast clearance ($t_{1/2} = 20$ min) from the occipital cortex, a region anticipated to be free of pathology. Conversely, regions expected to exhibit α -Syn pathology showed prolonged tracer retention ($n = 1$ for each case, $N = 1$). (B) time-SUVR curves reach a pseudo-equilibrium state at approximately 30 min after tracer injection. SUV_{bw}, standardized uptake value (body weight), SUVR, standardized uptake value ratio, Occ, occipital cortex.

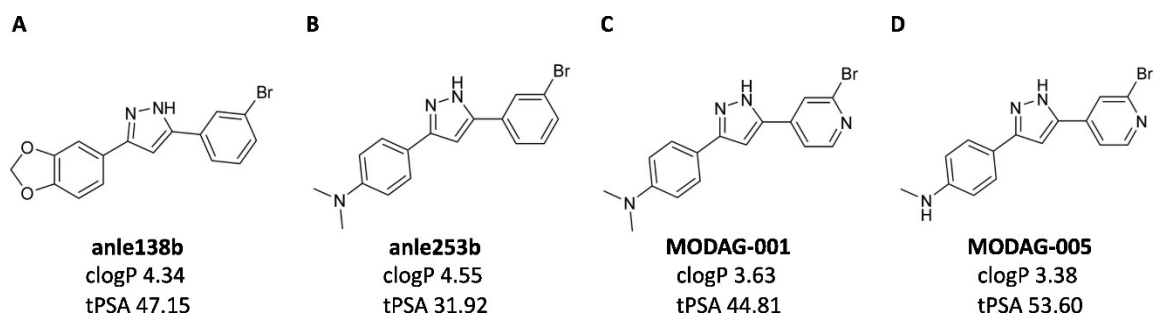


Fig. S20. Chemical structures of (A) anle138b, (B) anle253b, (C) MODAG-001, and (D) MODAG-005 with their calculated logP and topological polar surface area [\AA^2] values. Abbreviations: clogP, calculated logP; tPSA, topological polar surface area.

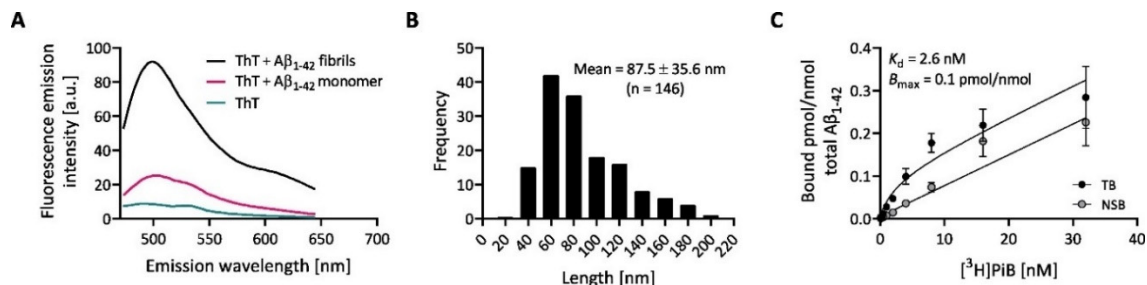


Fig. S21. A β ₁₋₄₂ fibrils were characterized through ThT fluorescence, electron microscopy and [³H]PiB binding assay. (A) High ThT fluorescence emission spectrum in the presence of A β ₁₋₄₂ fibrils compared to in the presence of monomers or ThT only (*n* = 1). (B) Length measurement and distribution of A β ₁₋₄₂ fibrils assessed from the negative stain electron microscopy images (mean length = 87.5 ± 35.6 nm from 146 measurements). (C) [³H]PiB saturation binding assay confirming good binding to A β ₁₋₄₂ fibrils, with a *K_d* of 2.6 nM and a *B_{max}* of 0.1 pmol/nmol (*n* = 1 biological replicate, *N* = 1 technical replicate). The points in C are the mean ± SD. Abbreviations: A β ₁₋₄₂, β -amyloid₁₋₄₂; NSB, non-specific binding; SB, specific binding; TB, total binding; ThT, thioflavin T.

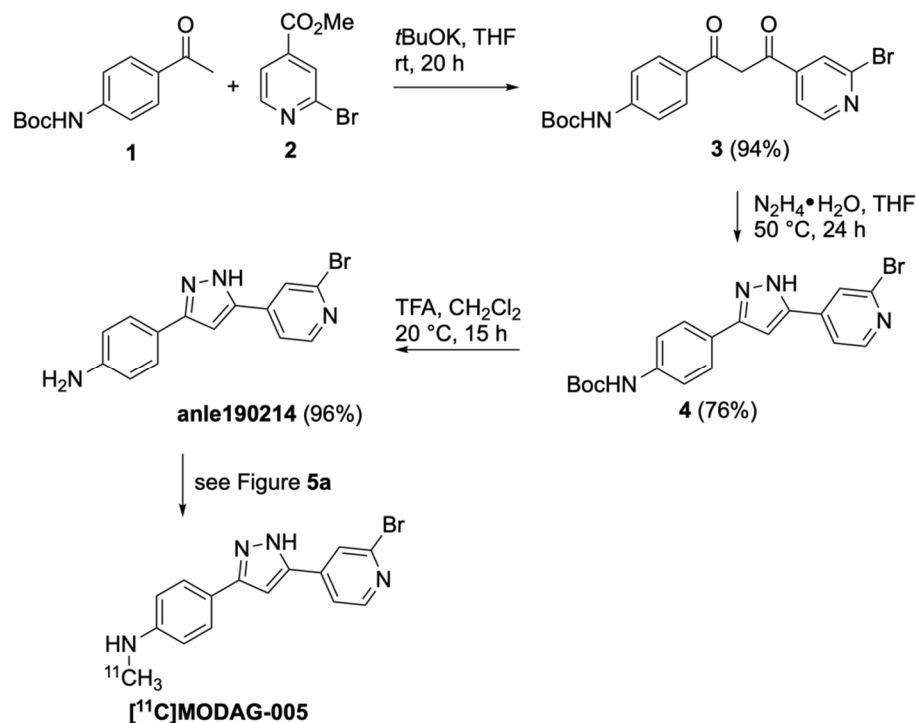


Fig. S21. synthesis of the precursor anle190214

Table S1 – Table S3

Table S1. Overview of the human brain sections used in the (micro)autoradiography experiments and immunofluorescence or immunohistochemistry validation.

Donors	Region	Age at death (years)	Sex	PMI (hour)	LBD (Braak)	AD (Braak & Braak)	AD (Thal)	Pathology		
								α -Syn	A β	pTau
MSA1	CB	64	F	52	0	I	1	+++	-	-
MSA2	CB	54	M	71	0	0-I	0	+++	-	-
Control1	CB	76	F	26	0	III	3	-	-	-
Control2	CB	66	F	27-39	0	I	3	-	-	-
PD	FC	79	F	26	6	IV	3	+++	++	+
AD	FC	70	M	24	0	VI	5	-	+++	+++
PSP	FC	66	M	7	0	0	0	-	-	+++
Control3	FC	64	F	39	0	0	0	-	-	-

The number of “+” symbols indicates an increasing degree of pathology in the particular region analyzed from low (+), moderate (++) to severe (+++) pathology; “-” symbolizes the absence of pathology. Abbreviations: A β , β -amyloid; α -Syn, α -synuclein; AD, Alzheimer’s disease; CB, cerebellum; Ctrl, control; F, female; FC, frontal cortex; LBD, Lewy body dementia; M, male; MSA, multiple system atrophy; PD, Parkinson’s disease; PMI, post-mortem interval; PSP, progressive supranuclear palsy; pTau, phospho-Tau.

Table S2. [¹¹C]MODAG-005 radio-metabolite quantification of brain and plasma samples at 5 and 15 minutes after injection in mice (n = 3 per time-point) and rats (n = 1 per time-point).

	<i>M1 (t_R 2.0 min)</i>		<i>M2* (t_R 3.9 min)</i>		<i>P (t_R 6.1 min)</i>	
	<i>%</i>	<i>%ID/volume or weight</i>	<i>%</i>	<i>%ID/volume or weight</i>	<i>%</i>	<i>%ID/volume or weight</i>
Mice						
<i>Brain, 5 min</i>	4.1 ± 1.1	0.5 ± 0.1 [#]			96 ± 1.1	13 ± 6.0 [#]
<i>Brain, 15 min</i>	21 ± 3.1	1.0 ± 0.2 [#]			79 ± 3.1	4.3 ± 1.6 [#]
<i>Plasma, 5 min</i>	40 ± 2.9	1.1 ± 0.4 ⁺	32 ± 1.5	0.9 ± 0.4 ⁺	29 ± 3.1	0.9 ± 0.4 ⁺
<i>Plasma, 15 min</i>	44 ± 11	1.2 ± 0.4 ⁺	33 ± 3.7	1.0 ± 0.4 ⁺	22 ± 7.6	0.6 ± 0.2 ⁺
Rats						
<i>Brain, 5 min</i>	9.0	0.3 [#]			91	3.0 [#]
<i>Brain, 15 min</i>	36	0.2 [#]			64	0.3 [#]
<i>Plasma, 5 min</i>	28	0.3 ⁺	36	0.4 ⁺	36	0.4 ⁺
<i>Plasma, 15 min</i>	34	0.4 ⁺	47	0.5 ⁺	20	0.2 ⁺

Data are the mean ± SD. Abbreviations: M1, metabolite 1; M2*, mixture of various metabolites; P, parent compound; t_R, retention time; %ID, % injected dose; #, per g brain tissue; +, per plasma in one mL blood.

Table S3. [¹¹C]MODAG-005 radio-metabolite quantification of plasma samples at 5, 15, 30, 45 and 60 minutes after injection in cynomolgus macaque (n = 2).

	<i>M1 (t_R 2.3 min)</i>	<i>M2* (t_R 6.6 min)</i>	<i>P (t_R 9.2 min)</i>
Cynomolgus macaque	%	%	%
<i>Plasma, 5 min</i>	19 ± 0.7	3.9 ± 1.0	74 ± 1.3
<i>Plasma, 15 min</i>	61 ± 1.6	6.9 ± 2.1	29 ± 0.3
<i>Plasma, 30 min</i>	70 ± 1.7	7.1 ± 0.9	18 ± 1.7
<i>Plasma, 45 min</i>	70 ± 1.4	7.5 ± 1.3	14 ± 1.0
<i>Plasma, 60 min</i>	67 ± 8.3	7.7 ± 3.2	8.6 ± 1.0

Abbreviations: M1, metabolite 1; M2*, mixture of various metabolites; P, parent compound; t_R, retention time.

Materials Design Analysis Reporting (MDAR) Checklist for Authors

The MDAR framework establishes a minimum set of requirements in transparent reporting applicable to studies in the life sciences (see Statement of Task: [doi:10.31222/osf.io/9sm4x](https://doi.org/10.31222/osf.io/9sm4x)). The MDAR checklist is a tool for authors, editors, and others seeking to adopt the MDAR framework for transparent reporting in manuscripts and other outputs. Please refer to the MDAR Elaboration Document for additional context for the MDAR framework.

For all that apply, please note where in the manuscript the required information is provided.

Materials:

Newly created materials	indicate where provided: page no/section/legend)	n/a
The manuscript includes a dedicated "materials availability statement" providing transparent disclosure about availability of newly created materials including details on how materials can be accessed and describing any restrictions on access.	Details are provided in the section "materials availability statement"	
Antibodies	indicate where provided: page no/section/legend)	n/a
For commercial reagents, provide supplier name, catalogue number and <u>RRID</u> , if available.	Details are provided in the Supplementary Materials - Materials and Methods - Immunofluorescence / Immunohistochemistry	
DNA and RNA sequences	indicate where provided: page no/section/legend)	n/a
Short novel DNA or RNA including primers, probes: Sequences should be included or deposited in a public repository.		/
Cell materials	indicate where provided: page no/section/legend)	n/a
Cell lines: Provide species information, strain. Provide accession number in repository OR supplier name, catalog number, clone number, OR RRID.		/
Primary cultures: Provide species, strain, sex of origin, genetic modification status.		/
Experimental animals	indicate where provided: page no/section/legend)	n/a
Laboratory animals or Model organisms: Provide species, strain, sex, age, genetic modification status. Provide accession number in repository OR supplier name, catalog number, clone number, OR RRID.	Details are provided in the Supplementary Materials - Materials and Methods - Animals	
Animal observed in or captured from the field: Provide species, sex, and age where possible.		/
Plants and microbes	indicate where provided: page no/section/legend)	n/a
Plants: provide species and strain, ecotype and cultivar where relevant, unique accession number if available, and source (including location for collected wild specimens).		/
Microbes: provide species and strain, unique accession number if available, and source.		/
Human research participants	indicate where provided: page no/section/legend) or state if these demographics were not collected	n/a
If collected and within the bounds of privacy constraints report on age, sex and gender or ethnicity for all study participants.	Details are provided in the Supplementary Materials - Materials and Methods - Human participants	

Design:

Study protocol	indicate where provided: page no/section/legend)	n/a
If study protocol has been pre-registered, provide DOI. For clinical trials, provide the trial registration number OR cite DOI.		/

Laboratory protocol	indicate where provided: page no/section/legend)	n/a
Provide DOI OR other citation details if detailed step-by-step protocols are available.		/

Experimental study design (statistics details)		
For in vivo studies: State whether and how the following have been done	indicate where provided: page no/section/legend. If it could have been done, but was not, write not done	n/a
Sample size determination	Information are provided in the Materials and Methods - Study Design Sample sizes were determined on the basis of prior studies or power calculation. Specific sample sizes and replicates for each experiment are provided in the corresponding figure legends or in Materials and Methods.	
Randomisation		/
Blinding	Information are provided in the Materials and Methods - Study Design (not done)	
Inclusion/exclusion criteria	Information are provided in the Materials and Methods - Study Design No data were excluded from the analyses, other than those that were justified for the study in α SYN(A30P) mouse model. See also Fig. S9B.	

Sample definition and in-laboratory replication	indicate where provided: page no/section/legend	n/a
State number of times the experiment was replicated in laboratory.	Information are provided in figure legends	
Define whether data describe technical or biological replicates.	Information on technical or biological replicates are provided in figure legends	

Ethics	indicate where provided: page no/section/legend	n/a
Studies involving human participants: State details of authority granting ethics approval (IRB or equivalent committee(s), provide reference number for approval.	Details are provided in the Supplementary Materials - Materials and Methods	
Studies involving experimental animals: State details of authority granting ethics approval (IRB or equivalent committee(s), provide reference number for approval.	Details are provided in the Supplementary Materials - Materials and Methods	
Studies involving specimen and field samples: State if relevant permits obtained, provide details of authority approving study; if none were required, explain why.		/

Dual Use Research of Concern (DURC)	indicate where provided: page no/section/legend	n/a
If study is subject to dual use research of concern regulations, state the authority granting approval and reference number for the regulatory approval.		/

Analysis:

Attrition	indicate where provided: page no/section/legend	n/a
Describe whether exclusion criteria were preestablished. Report if sample or data points were omitted from analysis. If yes report if this was due to attrition or intentional exclusion and provide justification.	No data were excluded from the analyses, other than those that were justified for the study in α SYN(A30P) mouse model based on immunohistochemistry analysis. See Fig. S9B.	

Statistics	indicate where provided: page no/section/legend	n/a
Describe statistical tests used and justify choice of tests.	Details are provided in the Materials and Methods - Statistical Analysis, and the statistical tests used are specified in the figure legends.	

Data availability	indicate where provided: page no/section/legend	n/a
For newly created and reused datasets, the manuscript includes a data availability statement that provides details for access or notes restrictions on access.	Details are provided in the section “materials availability statement”	
If newly created datasets are publicly available, provide accession number in repository OR DOI OR URL and licensing details where available.	Details are provided in the section “materials availability statement”	
If reused data is publicly available provide accession number in repository OR DOI OR URL, OR citation.		/

Code availability	indicate where provided: page no/section/legend	n/a
For all newly generated custom computer code/software/mathematical algorithm or re-used code essential for replicating the main findings of the study, the manuscript includes a data availability statement that provides details for access or notes restrictions.		/
If newly generated code is publicly available, provide accession number in repository, OR DOI OR URL and licensing details where available. State any restrictions on code availability or accessibility.		/
If reused code is publicly available provide accession number in repository OR DOI OR URL, OR citation.		/

Reporting

MDAR framework recommends adoption of discipline-specific guidelines, established and endorsed through community initiatives. Journals have their own policy about requiring specific guidelines and recommendations to complement MDAR.

Adherence to community standards	indicate where provided: page no/section/legend	n/a
State if relevant guidelines (e.g., ICMJE, MIBBI, ARRIVE) have been followed, and whether a checklist (e.g., CONSORT, PRISMA, ARRIVE) is provided with the manuscript.		/

Clinical Studies

Adherence to clinical standards	indicate where provided: page no/section/legend	n/a
State if relevant checklists are provided in the supplementary materials e.g., CONSORT for randomized controlled clinical trials, TREND for non randomized studies, REMARK for tumor prognostic studies, BRISQ for human biospecimens. Confirm that a CONSORT flow diagram is in Figure 1	(not applicable – the first-in-human imaging study was conducted following the regulations of the German Medicinal Products Act (“Arzneimittelgesetz” AMG §13(2b)))	/

Clinical Trial Registration	indicate where provided: page no/section/legend	n/a
Confirm that the clinical trial was pre-registered (before patient enrollment) and provide clinical trial registration number from ClinicalTrials.gov or other national registry	(not applicable – the first-in-human imaging study was conducted following the regulations of the German Medicinal Products Act (“Arzneimittelgesetz” AMG §13(2b)))	/

Ethics	indicate where provided: page no/section/legend	n/a
Confirm that informed consent was obtained from all human participants and state the details of the IRB or other authority granting ethics approval including approval reference number	Informed consents were obtained – Details are provided in the Supplementary Materials - Materials and Methods (IRB/ethics approval not applicable – the first-in-human imaging study was conducted following the regulations of the German Medicinal Products Act (“Arzneimittelgesetz” AMG §13(2b)))	

Demographics Reporting	indicate where provided: page no/section/legend	n/a
Study should follow authoritative standards for reporting demographics data. Descriptors for any demographic identities should be clear, unbiased, and up-to-date.		/

Identifiable images	indicate where provided: page no/section/legend	n/a
Authors should remove information from patient photographs that could be used to identify the patient. Where this is not possible, a written release from the patient must be provided.		/

Data Access	indicate where provided: page no/section/legend	n/a
Confirm that de-identified human data collected for the study will be made available to researchers/clinicians after publication. Confirm that		

the manuscript includes a Data and Materials Availability statement that provides details regarding data access or states restrictions on data access. If access to data is subject to a data transfer agreement (DTA) or data use agreement (DUA) provide a link to DTA/DUA or provide a copy of the DTA/DUA (which may be included as a supplementary materials file). If there are restrictions on data access, provide a statement regarding which data are restricted and the nature of the restriction.

--

--